Off-road Driving and Wildlife Trails Extraction from High Resolution Satellite Imagery:

A Curvelet Transform Based Approach

Shaoqing Lu
March, 2012

Course Title:	Geo-Information Science and Earth Observation for Environmental Modelling and Management
Level:	Master of Science (MSc)
Cource Duration:	September 2010 – March 2012
Consortium Partners:	Lund University (Sweden) University of Twente, ITC (the Netherlands)

Off-road Driving and Wildlife Trails Extraction from High Resolution Satellite Imagery:

A Curvelet Transform Based Approach

by

Shaoqing Lu

Thesis submitted to the University of Twente , Faculty of ITC in partial fulfilment of the requirements for the degree of Master of Science in Geo-information Science and Earth Observation, Specialisation: Environmental Modelling and Management.

Thesis Assessment Board

Chairman:	Dr. Albertus G. Toxopeus
External Examiner:	Dr. Valentyn A. Tolpekin
First Supervisor:	Dr. Tiejun Wang
Second Supervisor:	Prof. Dr. Andrew K. Skidmore

UNIVERSITY OF TWENTE.

FACULTY OF GEO-INFORMATION SCIENCE AND EARTH OBSERVATION

Disclaimer

This document describes work undertaken as part of a programme of study at the University of Twente, Faculty of ITC All views and opinions expressed therein remain the sole responsibility of the author, and do not necessarily represent those of the institute.

Abstract

Maasai Mara national reserve is considered as a natural ecosystem where off-road driving activities occur frequently. These activities have synergistic and cascading negative impacts throughout an ecological system especially to the wildlife. For proper monitoring and management, there is the need for information on extent and magnitude of off-road driving problem. This information is expensive, strenuous and time consuming to produce using conventional approaches. This research concentrates on extracting the off-road driving and wildlife trails automatically from GeoEye-1 high resolution satellite imagery. An innovative curvelet transform based approach is developed and implemented in Matlab. It is a multiple-stage framework which is composed of three main blocks: 1. Extracting the high-contrast curvilinear feature from curvelet magnitudes derived from the finer scale of curvelet coefficient. 2.Extracting the low-contrast curvilinear feature from a coarser scale curvelets and refine the shape by deformable active contour (snake). 3. Categorizing the extracted curvilinear feature into off-road driving and wildlife trail by a self-designed fuzzy logic inference system. For evaluating the extraction results and quantifying the performance of the extraction and categorization methods in terms of completeness, correctness, redundancy and categorical accuracy, manual digitizing of the trails according to visual interpretation are conducted and compared with the extraction results in a GIS environment. The results are promising with an overall accuracy of 90%, 75%, 4%, and 74% in terms of the above mentioned four quality measures respectively. Conclusion has been drawn that curvelet transform as the very powerful fundamental tool with its distinct mathematical properties is capable of dealing with the unprecedented extraction task assisting for a better understanding of the off-road driving activities and wildlife migration patterns in the study area.

Key words: Vehicle Trail, Trail Extraction; Curvelet Coefficient; Deformable Active Contour; Fuzzy Logic Inference; Image Analysis;

Acknowledgements

First of all, it is a great honour to be granted by Erasmus Mundus scholarship to attend this amazing GEM MSc. course. My very first appreciation goes to the Education and Culture DG, European Union.

From Lund University I learned all the basics on how to participate in team work and how to do presentations. I give my deepest gratitude to all the faculty members of NATEKO who have taught me and supported me. Further thanks go to Prof. Petter Pilesjö who assisted my orientation before and after I came to Sweden.

From the ITC where I started doing my thesis research I learned how to dedicate myself to contribute the world of science. I give my sincerest appreciation to my first supervisor Dr. Tiejun Wang. It is you who spent plenty of time training my scientific critical thinking, encouraging me when I was stuck on my research and proposing such an innovative and interesting research topic. Many thanks go to my second supervisor Prof. Andrew Skidmore for your inspiring thoughts on my research. Many of your comments to me or even to other people when they were defending their proposals and mid-term evaluation were beyond our own thinking box.

I gratefully acknowledge the support of ©GeoEye; GeoEye-1 satellite imagery courtesy of GeoEye Foundation which supplied us the imagery. Appreciation also goes to Dr. Jan de Leeuw and Dr. Mohammed Said from Consultative Group on International Agricultural Research (CGIAR), Kenya, for your effective cooperation on this research. Dr. Shadrack Ngene from Kenya Wildlife Service, thank you for providing the road network vector data of Maasai Mara National Revere.

It is really a unique experience attending the GEM course with all of you lovely GEMies from all over the world: Sweet couple Anna and Mauricio; Captain Alan; Igwe Arodudu; Amazing Kong, Mina, Giles, Martin and Fahmy; My Sis. Katarina; My Greek inlaw Christopher; My inlaw Ben, My inlaw Shadi and My inlaw Abellac. Thank you! Words can not explain all the happy moments we have spent together!

Special thanks to my inlaw, Abel Chemura! It is you who changed me from a little child to where I am now. Thank you for letting me know God, Hallelujah! I appreciate and treasure every single moment being with you. God bless you have a brilliant future!

Finally, I offer my greatest appreciation to my beloved parents!

Table of Contents

List of figures

List of tables

1 Introduction

1.1 Background

The rapid development of technology since the Industrial Revolution as well as the increase in human population, increases the numbers of ways and the intensity with which human beings affect the environment (Goudie, 2006). As one of the by-products of a highly developed society, a stronger demand for recreation and tourism has been generated. This contributes to one of the unprecedented ways of disturbing the ecosystem. Activities such as touring, hiking and passive mountain bike riding in grasslands have an impact where roads and trails cross the landscape in term of soil erosion (Wilson and Seney, 1994). It can also affect individuals, populations, and wildlife communities (Knight and Gutzwiller, 1995). Among all recreation and tourism activities, it is reported that off-road driving is the fastest growing one which occurs on public lands in developed countries such as the United States (Davenport and Switalski, 2006). Since it has gained popularity in 1970's, scientists have already realized and warned of the adverse impacts of off-road vehicles (ORVs) (Busack and Bury, 1974; Eckert et al., 1979; Webb et al., 1978; Vollmer et al., 1977).

Uncontrolled use of all-terrain vehicles and other ORVs has a synergistic and cascading impact throughout an ecological system as well as in various aspects of different types such as soil compaction, vegetation degradation and disturbing the wildlife (Crist, 2006; Goudie, 2006). However, compared to the massive impacts of ORVs to the natural environment, efforts to control this activity are fragmented and underfunded (Bury, 1980).

Lack of funding, foresight, dedication, collaboration and governmental support are the main factors that contribute to the dramatic expansion of these kinds of activities. Since 1970's, in spite of over 35 years' massive scientific studies, sufficient evidence and support have been provided to carefully control and to manage the ORVs on public lands, it still remain largely unmanaged and getting worse (Kassar, 2005). Nonetheless, there is no adequate evidence to show the severity, extent and magnitude of ORVs activities and it is a common sense that we, as human-beings will only take care of what we know and dismiss or ignore what we have not seen or recognized. Thus, it is important to show the general public and land management agencies that the status of ORVs activities happening around us.

Many hundreds of papers about the physical and ecological effects of roads and ORVs have been published (Taylor, 2002; Wildlands, 2011). However, few are related to the novel methodology of quantifying detailed spatial extent and magnitude of ORVs activities specifically. It is crucial to show people where and what is the magnitude of ORVs activities currently happening within a certain scale area not only because it will benefit the management agencies to make polices but also for the public to realize that this is a serious problem. Based on the information about the spatial distribution and how serious the activities take place, land agencies, other responsible organization or relevant research groups can then effectively fulfil their legal and ethical obligations to control ORVs use and prevent the problem from continuing to worsen.

Efforts have been made to examine off-road driving trails (hereinafter referred to as "vehicle trails") based on ground surveys (Walpole, 2003; Wilson and Seney, 1994). Nevertheless, ground surveys are not only time consuming but also costly in terms of human resources. Considering most of the regions to be investigated are roadless and in a natural environment, additional adverse impacts will be created especially when the regions are ecologically vulnerable. As an alternative, aerial photography-based investigation as a better approach conquers above mentioned shortcomings of ground based survey. Digitized off-road driving trails from aerial photography were analysed by Griggs and Walsh (1981) and Priskin (2003) to evaluate the environmental impacts. However, with a scaled up study area and a higher density trails distribution, the manual labour for digitizing will be increased tremendously making this approach time consuming (Laptev et al., 2000) and tedious to conduct.

Photogrammetry and computer vision technologies have been used for automated extraction of man-made objects especially in the last two decades. This is also a multi-discipline research topic where computer vision, earth observation technology and machine learning are closely cooperated. Since the first attempt of road extraction from Landsat-1 MSS tried by Bajcsy and Tavakoli (1976), a range of techniques have been developed from low-level approaches such as mathematical morphology (C. Zhang and Baltsavias, 1999; Zlotnick and Carnine, 1993) to high-level methods such as knowledge representation (Baltsavias, 2004) and object-based analysis (Blaschke, 2010). Over 250 references in road extraction have been reviewed by Mena (2003). Quite a lot of them provide promising results in different context although maturity of a general approach still do not exist (Mohammadzadeh et al., 2009). In addition to that, few studies attempted to undertake extracting curvilinear features

such as vehicle trails with such a narrow width associated with the variability of reflectance property.

However, more recently, high spatial resolution commercial satellite images with multiple spectral channels such as GeoEye, QuickBird, IKONOS provide a very high geometric precision up to 0.41 m. With this high resolution data associated with the foundation of previous exhaustive studies on man-made roads extraction, the potential for automatic and accurate detection of vehicle trails whose width is about 1.5 m will be promising.

Maasai Mara national reserve is considered as a natural ecosystem where off-road driving activities occur frequently (Ikiara and Okech, 2002). Several factors are worthy to be raised as the unique advantage of choosing Maasai Mara as a representative study area for developing the trail extraction methods. As a savanna system, the landscape is open which makes it possible for the vehicle trails to be detected by optical remote sensing imagery. Likewise, the vehicle trails' condition are complicated due to the high variability of the frequency the trails have been used. This makes the trails' radiometric property different. Furthermore, the discontinuous and ambiguous visual characteristics make the case even more complicated. Finally, as a site where the spectacular annual great wildebeest migration occurs, wildlife trails can be a big noise to the vehicle trails. Based on this "worst scenario case", the extraction method developed from Maasai Mara will be more likely applicable to other area in the rest of the world. In addition, wildlife, as one of the components in the ecosystem, is very vulnerable from the negative effects by ORVs. Both direct and indirect impacts are addressed by Kassar (2005). Thus, reasons are sound for extracting wildlife trails not only because it contribute to the ecological research but also benefit the park management. Photogrammetry and computer vision community will also benefit considering it as a technical challenge.

1.2 Research problem

Automatically extracting objects from digital image is not only technically and scientifically challenging in the photogrammetry and remote sensing community as an application of earth sciences but also as a broad general issue under computer vision and image analysis for decades (Mena, 2003). For the time being, curvilinear feature extraction still follows an "ad-hoc multistage approach" (Mnih and Hinton, 2010). Thus, simply applying the current methods for extracting man-made roads to the vehicle trails whose characteristics are different may not be robust. Regardless of the fact that they are

both curvilinear features, vehicle trails are situated in natural environment and have different backgrounds and contexts from previous studies that focused on extraction of man-made roads. Hence, remodelling the curvilinear feature and their relations with the background objects is crucial. In addition, more specifically, the wildlife trails in Maasai Mara could be a big challenge considering them as noise to vehicle trails. However, it is also an opportunity for extracting the wildlife trails once there are separated from the vehicle trails so that further spatial pattern could then be analysed for later applications.

Once the extraction work has been done, useful information can then be mined. Providing quantitative information about the magnitude of off-road driving activities to the local authority as a by-product of the extracted trails could be misleading when an inaccurate result that contains both commission and omission errors occurs. A complete and systematic evaluation scheme has been adequately proposed to validate the road extraction results (Heipke et al., 1997). On the other hand, observed from a high resolution image, vehicle trails vary significantly from one to another due to complex factors like the uneven frequency of usage, the underneath soil types and soil moisture. Hence, to define and model different types of trails are not only a necessary work but also a key stage of evaluation. Based on this information, a strategy can thus be developed to categorize the trails extracted into different types.

1.3 State of the art on curvilinear feature extraction

Although studies on the target objects to be extracted in this research have never been discussed to the best knowledge of the author based on a massive literature review, it can be considered as curvilinear feature extraction from digital images which shares the common topic in computer vision and image analysis. Intensive research for decades on man-made road extraction as a representative of photogrammetry and remote sensing application; elongated features in images of intracellular and multicellular structures extraction as a typical application of medical image analysis both indicates that curvilinear feature extraction is still far from the goal of a fully automated system (Geback and Koumoutsakos, 2009; Mirnalinee et al., 2011). The following overview of the current research status is mainly based on man-made road extraction cooperated with a few studies related to curvilinear feature extraction from medical images.

1.3.1 Radiometric feature-based approaches

Image pixel value statistics have been analysed using Iterative Self-Organizing Data Analysis (ISODATA) algorithm by Koutaki and Uchimura (2004), Zhang et al. (2000) and Zhang et al. (1999). Considering S component in an image IHS (Intensity, Hue and Saturation) colour space, (Green-Red) / (Green+Red) from the RGB colour space and the brightness, during the iteration process current clusters are separated and merged. Fuzzy clustering (Dell'Acqua and Gamba, 2001; Reigber et al., 2007) and genetic algorithm (Byoung-Ki et al., 2002; Yuan et al., 2007) have also applications in road extraction.

Morphological operations have been applied to avoid noises potentially being classified as road features (C. Zhang and Baltsavias, 1999). The combination of different morphological operations made the gap of road segment connected grows the incomplete segment as well as eliminated the non-road features. (Zhu et al., 2005)

Template matching selects the candidate of road segment by calculating the similarity between the template profile and the image (Vosselman and Knecht, 1995). Bajcsy and Tavakoli (1976) used 52 predefined template to compare with the binary segmented image and selected the road candidate followed by filtering based on the constraints of curvature and length.

Edge detection is the procedure of detecting the contrast of the image intensity. The contrast occurs in the boundaries of features within an image on which human beings perceive the different kinds of features based. The boundaries of features in an image are a step change instead of a rapid one. The position can be detected by analysing the differentiation of one pixel towards its neighbours.

1.3.2 Geometric feature-based approaches

Snake has been widely used in feature extraction from images by Kass (1988) as an energy minimization framework to archive of detection of edges, lines, and subjective contours; motion tracking; and stereo matching. As an active contour approach, it has been adapted into Ribbon snake (Fua and Leclerc, 1990), Ziplock snake (Neuenschwander et al., 1997) and Quadratic snake (Marikhu et al., 2007) for extracting road network in images.

Hough transformation uses a parametric approach to transfer the image into the parameter space. By searching for the peaks in the

parameter space, linear features are thus detected. Lee and Moon (2002) extracted linear features by Hough transformation and tested them on images from different sources including both optical and radar images.

Template matching is also used to extract features in the image. A template is a description of the general properties of the feature of interested. It is fixed in terms of properties such as size, shape. By moving the template, features are identified according to a certain kind of similarity measure (e.g., correlation coefficient) (Suetens et al., 1992). Gruen and Li (1997) used a least-square template matching approach to fit roads a Snake using a deformable contour as the template.

1.3.3 Frequency domain and multiple scale-based approaches

The width of roads appear in the imagery depends on the spatial resolution of the imagery and the actual functionality of the roads in reality. Same roads show different width in imageries of different spatial resolution; same imagery contains roads of different width. The homogeneity of the roads varies in imageries. It is the fact that roads can be best extracted in different scales (Heipke et al., 1995). The resolution affects the effectiveness of the extraction (Tieling et al., 2002).

Wavelet transformation for imagery transforms the image into the frequency domain and obtains wavelet coefficients at different scales. By analysing the coefficients in different scales, road network from remote sensing images was detected well from IRS and IKONOS imagery (Q. Zhang and Couloigne, 2004). Pyramids layers were generated by wavelet transformation to degrade the scale of images (Couloigner and Ranchin, 2000) to extract the urban streets.

The problem with the wavelet is that it extracts frequencies only in three directions (vertical, horizontal and diagonal) and only handles point discontinuities along the edges. It fails to extract curve discontinuous. In order to overcome the disadvantages in wavelets, Ridgelets are being proposed (Candès, 1998). Ridgelets extract frequencies of an image in all directions. It represents lines and singularities across the lines using fewer coefficients. However, most of the natural images contain curves rather than lines. So, a transform which represent curves will better represent the natural images rather than lines. Curvelets are used to better represent curves. Curvelet transformation provides a multi-scale representation

developed by Candès and Donoho (2004). It is a higher dimensional generalization of the Wavelet transform designed to represent images at different scales and different angles. Because of this higher dimensional property of curvelets, it is useful for denoising images with edges and for extracting edges (Geback and Koumoutsakos, 2009).

1.4 Research objectives

The aim of this research is to extract the predefined types of off-road driving and wildlife trails from high resolution GeoEye-1 satellite imagery using a curvelet transform-based approach.

To achieve the main target, the following specific objectives need to be addressed.

1) To extract the relatively high-contrast curvilinear features by applying the non maximal suppression algorithm to the finer scale curvelet coefficients.

2) To extract the relatively low-contrast curvilinear features by applying the curvelet-based snake algorithm to the coarser scale curvelet coefficients.

3) To categorize the extracted curvilinear features into wildlife trails and vehicle trails using fuzzy logic inference system.

4) To assess the accuracy of extracted wildlife and vehicle trails in both geometric and categorical aspects.

1.5 Structure of the thesis

In chapter 1, the background of ecological concern about the off-road driving and wildlife trails is raised and state of the art on image analysis techniques about the extraction is reviewed. The history of frequency domain and multi-scale based approaches' family is addressed followed by research objectives.

In chapter 2, the study area and available remote sensing satellite imagery data is described. The experimental data is selected and interpreted. The software development environment is introduced.

In chapter 3, the methods that are used in this thesis are explained and justified. Detailed descriptions of the theoretical background as well as the implementation of the technique used to extract the trails

in each processing step are presented. Finally, the approach for the validation of the final results is addressed.

In chapter 4, the performance of the developed extraction system is assessed. The results are presented and compared both visually and statistically with the manually digitized reference data. Overall statistical results of the performance are shown in the end of the chapter.

In chapter 5, numbers of issues related to the entire research are raised and discussed. The strength of the developed methods and the way to improve the results from sources of error perspective are discussed comprehensively.

In chapter 6, the conclusions and outlook are presented.

2 Study area and materials

2.1 Study area and image data

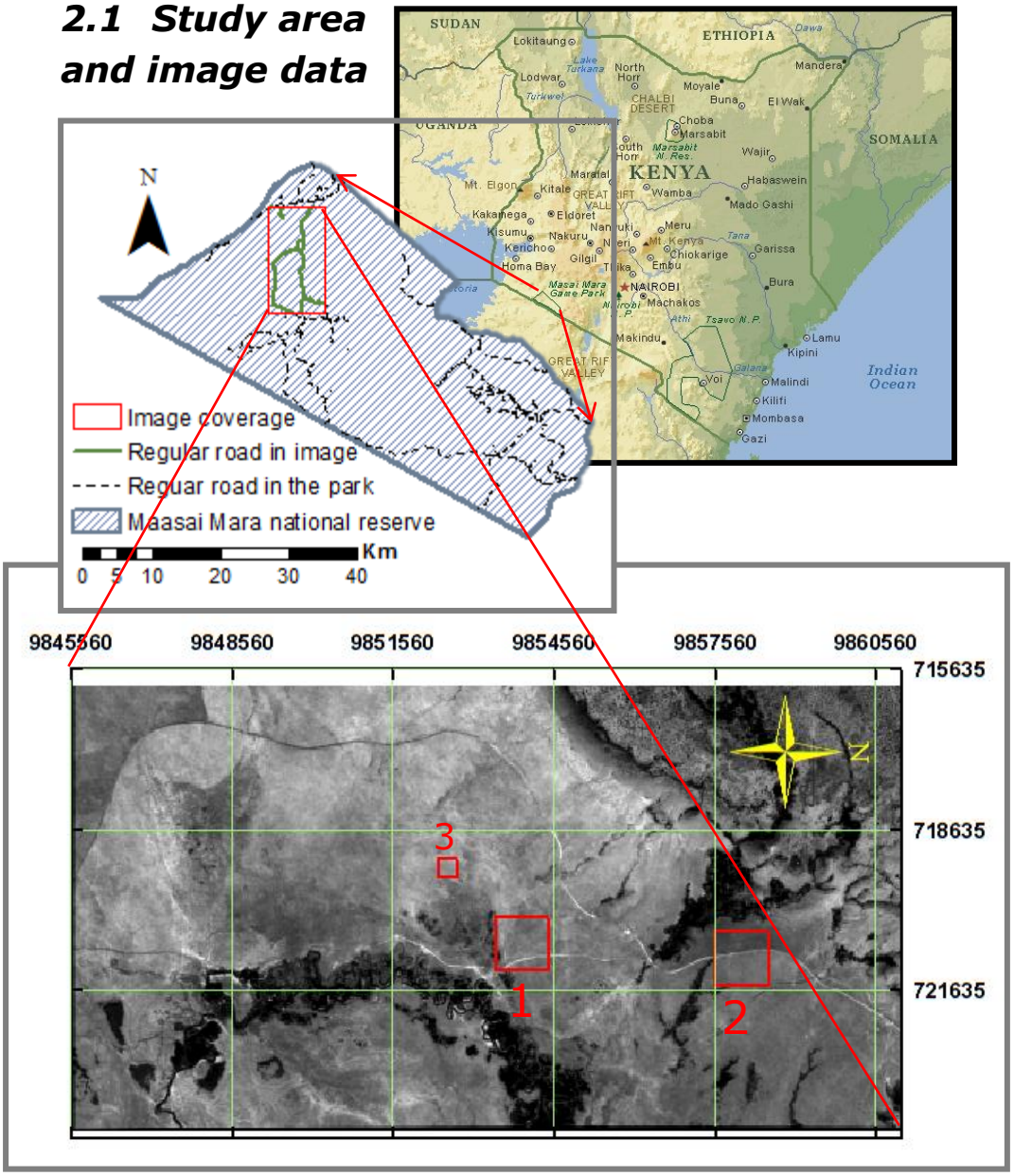

Figure 2.1 Location of study area, available regular road data in study area (source: Kenya Wildlife Service) and GeoEye-1 satellite image data (acquired on 11/08/2009 provided by ©GeoEye; GeoEye-1

satellite imagery courtesy of GeoEye Foundation) with 3 red window of selected test data.

Maasai Mara National Reserve is located in Narok District, Rift Valley province, Kenya (see Figure 2.1). It covers some 1,510 km^2 (Walpole, 2003) in south-western Kenya where the so called 7th wonder in the world, the great migration of wildebeests is located. Tourism is prospective there and generates millions of dollars annually for the treasury, and literally thousands of Kenyans are employed in the wildlife-based tourism industry throughout the country (Sindiga, 1999). A trend of increasing off-road driving activities was observed in Kenya (Walpole, 2003). The GeoEye-1 image available covers a study area from 34 ° 56 ′ 27.31 ″ E to 35 ° 00 ′ 56.69 ″ E and 1 ° 15 ′ 18.90 ″ S to 1 ° 23 ′ 46.90 ″ S in west part of the reserve shown in Figure 2.1.

GeoEye-1 satellite image was acquainted on 11th August, 2009 and was geo-referenced to the projection system of UTM Zone-36 South with the geodetic datum of WGS-84. It covers an area of 8304 by 15598 meters east-west wards and north-south wards respectively. Spatial resolution and other key features for each band can be found in the following Table 2.1.

Table 2.1 General characteristic of GeoEye-1 imagery

Band	Spectral Range (nm)	GSD (Nadir) (m)	Pixel Size (m)
Panchromatic	450-800	0.41	0.5
MSS Blue	450-510	1.65	2.0
MSS green	510-580	1.65	2.0
MSS Red	655-690	1.65	2.0
MSS Near Infrared	780-920	1.65	2.0

In this research, only panchromatic band is used for its highest spatial resolution of 0.5 meter. Three windows of test data are selected which all contains regular roads, vehicle trails and wildlife trails as shown in the red window of the satellite image in Figure 2.1. Detailed information for all the three windows are described in the following section.

Regular road information is provided by Kenya Wildlife Service in the format of vector road network layer.

2.2 Test data sets

Three test data sets are selected preparing for test the performance of the approach developed.

Window 1:

This test site covers a 1000 m by 1000 m area from 720261 m to 721261 m East-West and 9853462 m to 9854462 m South-North in an UTM 36s Zone projection system with the WGS 84 geodetic system.

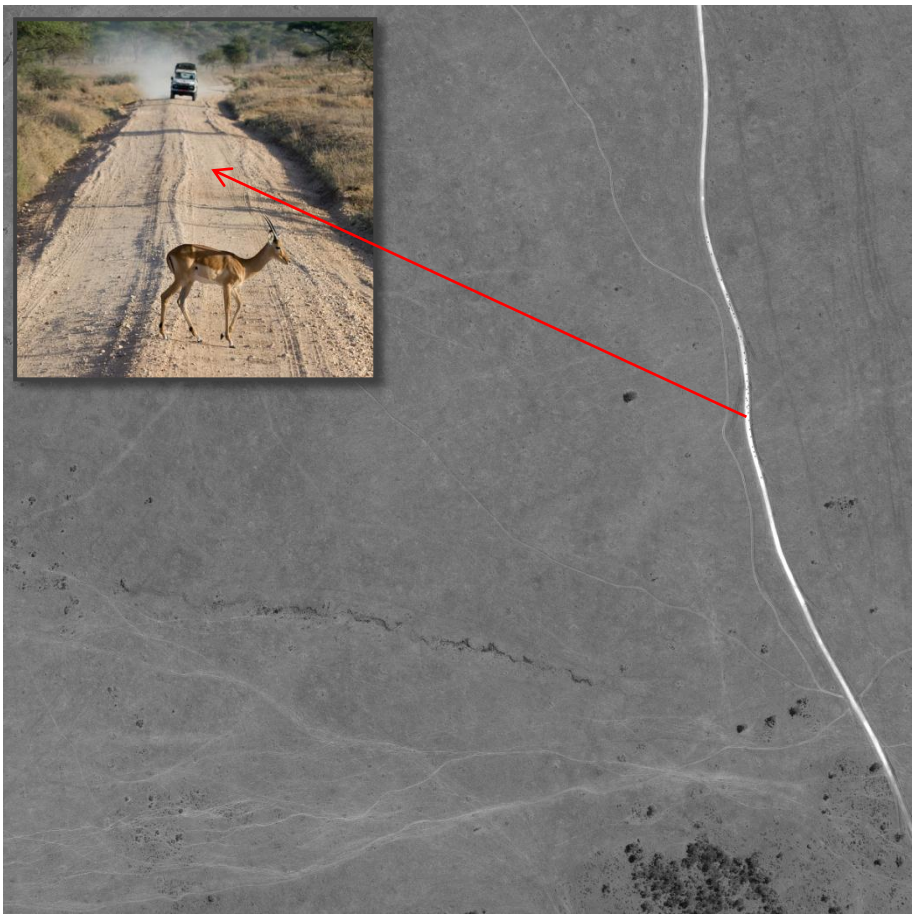

Figure 2.2 GeoEye-1 image for test data set 1 and corresponding illustrative ground photograph

Window 2:

This test site covers a 1000 m by 1000 m area from 720536 m to 721536 m East-West and 9857558 m to 9858558 m South-North in an UTM 36s Zone projection system with the WGS 84 geodetic system.

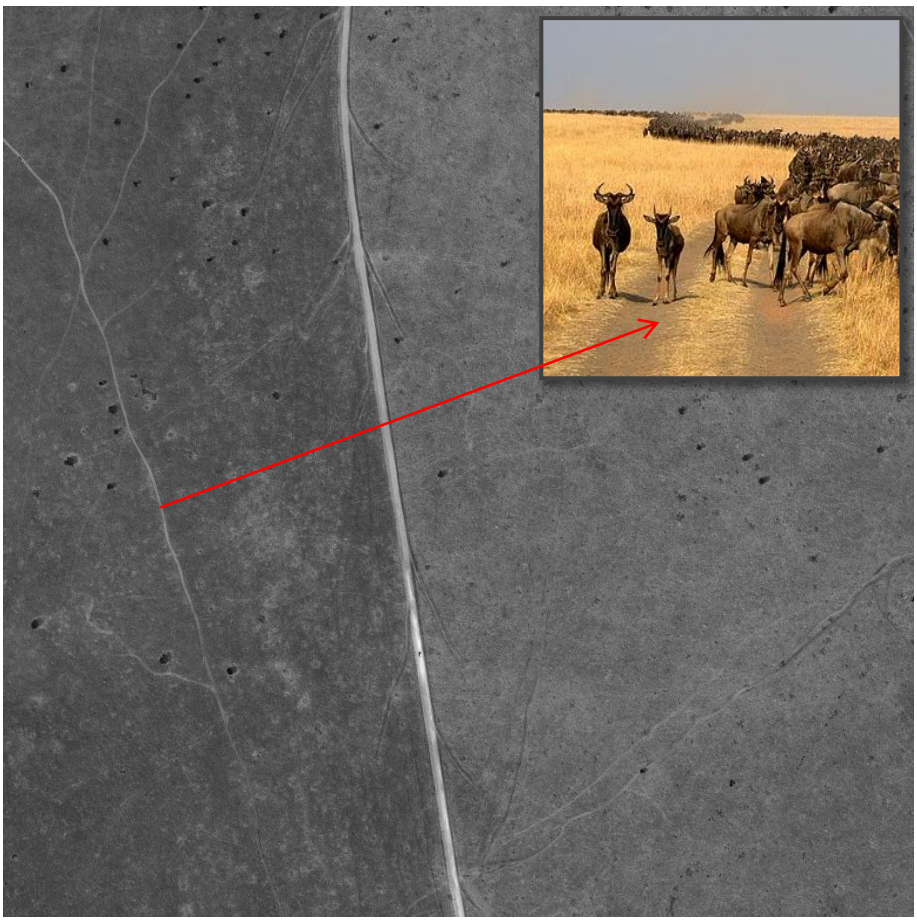

Figure 2.3 GeoEye-1 image for test data set 2 and corresponding illustrative ground photograph

Window 3:

This test site covers a 350 m by 340 m area from 719171 m to 719521 m West-East and 9852403 m to 9852743 m South-North in an UTM 36s Zone projection system with the WGS 84 geodetic system.

Figure 2.4 GeoEye-1 image for test data set 3 and corresponding illustrative ground photograph

2.3 Software development environment

Dealing with digital image, both professional remote sensing image processing software packages and integrated development environment for programming are used for the implementation and integration of different algorithms; Geographical information system will also be employed to assist for extraction accuracy evaluation.

Erdas Imagine 2011:

For remote sensing imagery data preprocessing such as examining the data and image enhancement.

Matlab 2007b:

For developing the image processing computer program for extracting vehicle and wildlife trails.

ArcGIS 9.3:

For accuracy assessment of the vehicle trails and wildlife trails extraction results.

CurveLab 2.1.2:

A Matlab toolbox implementing the Fast Discrete Curvelet Transform. It is freely available at http://www.curvelet.org implemented by the Curvelet.org team: Emmanuel Candes, Laurent Demanet, David Donoho and Lexing Ying.

CurveletUtils:

A Matlab toolbox providing a high-level interface handling curvelet coefficient and extracting curvilinear features by non-maximal suppression approach on curvelet magnitude. It is freely available at http://chaton.inf.ethz.ch/software implemented by Computational Science and Engineering Library in ETH Zurich.

3 Methods

3.1 Approach outline

For this research, three dominant modules are designed along with the pre-processing stage. Due to all kinds of the complexity of the study area, the trails appearing on the image are not always the same visually but come with a rich variability. Thus, the first part is to define the types of the trails to be extracted from the satellite image and to examine their properties in terms of geometry and radiometry carefully. The second part is the development of image processing and analysis algorithm in Matlab to extract the object of interest from the image. Validating the results is conducted in ArcGIS in the final module.

The pre-processing stage is about some low-level image enhancement. In this research, only the panchromatic band of the satellite image is used. The image enhancement procedure is to reduce the noise and enhance the contrast of the image. This stage is conducted in Erdas to form a better contrasted image to understand the characteristic of the wildlife and vehicle trails in study area.

The modelling module is to understand the properties of the object being extracted at a conceptual level thus to form the prior knowledge for the next module. For decades researchers have been dealing with man-made roads extraction and have formed several general characteristics of them both in geometric and radiometric manner such as the certain width and curvature or the homogeneity of the high reflectance (Mirnalinee et al., 2011). However, similar kinds of characteristics for vehicle and wildlife trails have not yet been summarized and generalized which can be done by visual interpretation. Further investigation can be performed by spatial profile analysis to model the spectral content of the trails as the previous studies did for man-made road extraction.

The image processing, analysis and understanding module plays the core role of the whole extraction framework. Due to the existence of the complex phenomena for different kinds of trails, it is almost impossible to consider and model all these situations and fit them into a unified pipeline. Thus a hierarchical and multiple stages, consisting of the curvelet-based edge detection, curvelet-based snake and fuzzy logic inference system approach to obtain descent results with a satisfied quality is proposed in this research.

The last module is to evaluate the quality of the results extracted in this proposed methods. Since in this research trails are not only extract but also recognized in a categorical perspective, the evaluation scheme including completeness, correctness and redundancy proposed by Heipke, et al. (1997) is not sufficient. A categorical quality is proposed for assessing the performance of the fuzzy logic inference system. Manual digitizing the vehicle and wildlife trail as reference data from the original panchromatic image is based on the prior knowledge developed in modelling module. For each type of trails, all above mentioned measures are calculated as the evaluation of the system.

In general, the very brief methodology flow chart is shown in Figure 3.1.

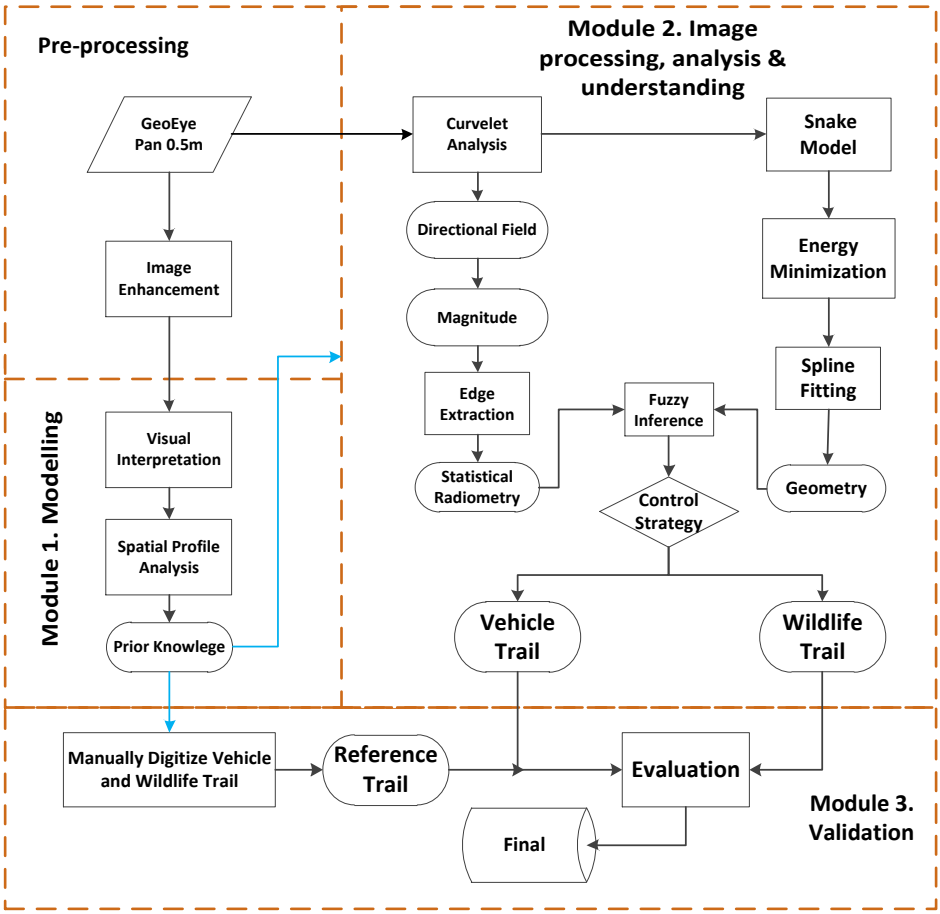

Figure 3.1 Overall methods flow chart

3.2 Modelling

Modelling is the premise of extracting any object from a digital image and the object of interest has its own unique properties that make it distinguishable from other neighbouring context objects. Only through studying and investigating those properties carefully enough can we extract them not only possibly but also efficiently. Thus, to form a prior knowledge towards the vehicle and wildlife trail is crucial.

The trail model defined here is an adaption from man-made road model. A road model has been conceptually established which comprises explicit knowledge about geometry, radiometry, topology and context relation (Hinz et al., 1999). Likewise, model for vehicle and wildlife trails is illustrated in Figure 3.2 but without taking topology into consideration.

Different types of trails appear differently on the GeoEye-1 imagery in our study area as shown in Figure 3.2. The conceptual model can thus be established to link the image and reality together by both the geometric and radiometric characteristics but within two different scales as illustrated by Figure 3.2. The geometry and radiometry level is an intermediate level which represents the 2D-shape of an object as well as its material (Clement et al., 1993). The idea behind this level is that in contrast to the image level it describes objects independently from sensor characteristics and viewport. The fine scale gives more detailed information from which a parallel double thin line can be found; the coarse scale adds global information. Because of the abstraction in coarse scale, additional correct hypotheses for trails can be found while details, like exact width and position from fine scale are integrated. In this way the extraction benefits from both scales.

The inner ring represents the real world objects while the outer one represents the corresponding phenomena in a satellite image. Two rings in the middle is the abstracted description in both coarse and fine scale as the bridge linking the inner (the reality) and outer (the image) one.

The other two modules (image processing and evaluation) are the implementations of the concept developed from the first stage which will be sufficiently described in the following section.

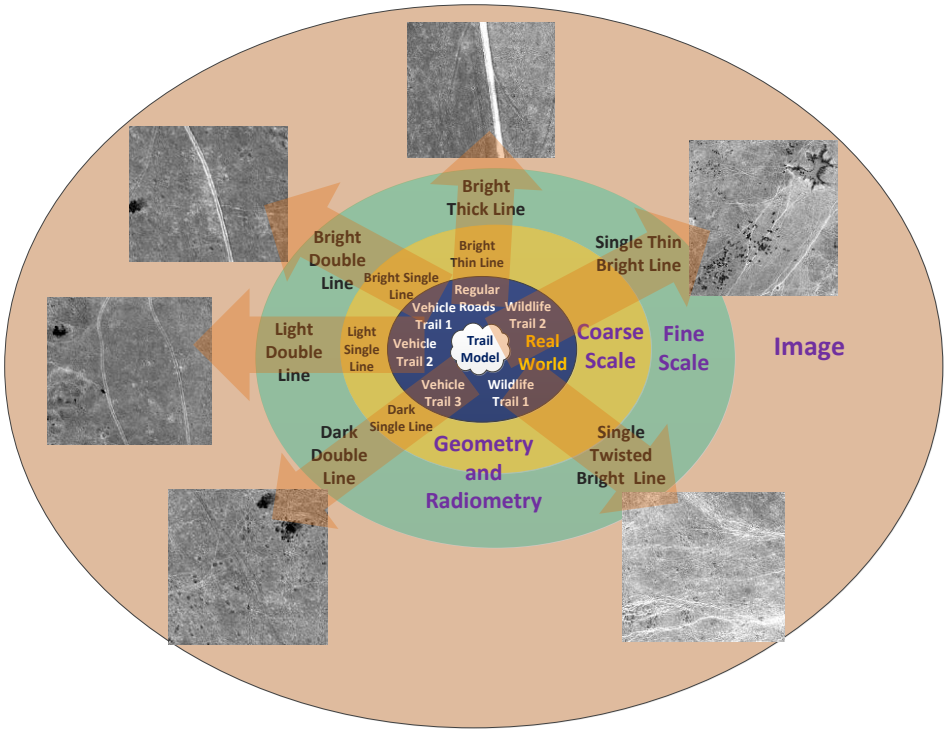

Figure 3.2 Conceptual model of different kinds of trails

To be more specific, spatial profile for each type of trail is analysed in Erdas. Vehicle trail 1 and 2 in Figure 3.2 are generalized as vehicle trail type 1 in the following modelling; wildlife trail 1 and 2 in Figure 3.2 are merged as one model.

1. Regular road appears in the image as a unified wide line. It has an extremely high spectral contrast to its background as shown in Figure 3.3. The profile can thus be modelled by piecewise linear equation.

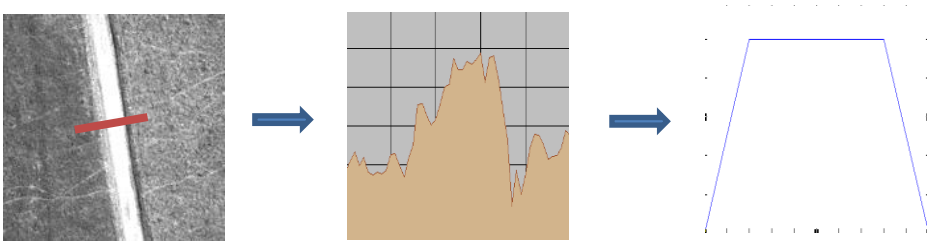

Figure 3.3 Regular road and its cross section spatial profile

2. Vehicle trail type 1 appears in the image as double line track. It has a relatively high spectral contrast to its background as shown in Figure 3.4. The double peak shape profile can be modelled by a quadratic polynomial equation.

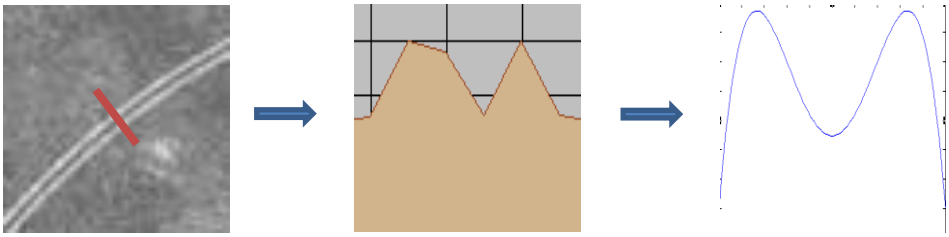

Figure 3.4 Vehicle trail type 1 and its cross section spatial profile

3. Vehicle trail type 2 appears in the image as a dark line. It has a relatively low spectral contrast to its background as shown in Figure 3.5. The valley-like profile can be model by a parabola.

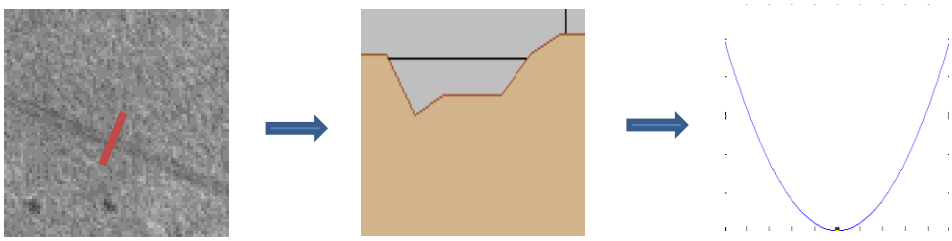

Figure 3.5 Vehicle trail type 2 and its cross section spatial profile

4. Wildlife trail appears in the image as multiple twisted threads. It has a relatively low spectral contrast to its background as shown in Figure 3.6. The profile appears random which is not possible use any mathematical equation to model.

Figure 3.6 Wildlife trail and its cross section spatial profile

However, the concentration in this research is only on vehicle trails and wildlife trails. Regular road is beyond the scope but can be dealt with by utilizing the road data from the park management.

3.3 Image analysis

This module is the most important part of the whole research which is composed of three major blocks. Firstly, the curvelet-based edge detection is designed to extract the most significant curvilinear features in the image including both high-contrast double line vehicle and wildlife trails. Secondly, the low-contrast off-road trails which are not detected in the first stage are extracted by curvelet-based snake approach. Finally, the trails extracted from both stages are combined together by applying mathematical and to categorize them, fuzzy logic inference is applied to fulfil the task.

3.3.1 Curvelet-based edge detection

❖ Continuous curvelet transform

Curvelet transform was first introduced by Candès and Donoho (1999). It was motivated by the problem of finding efficient representation of objects with discontinuities along curves and of compression of image data.

The new frame work of curvelet transform developed by Candès and Donoho (2004) is also called the second generation of curvelet transform which is an upgraded version of the previous one. Unlike the first generation, the curvelet transform under the new frame work does the multi-scale analysis directly in the frequency domain while in the first generation, the complicated ridgelet transform analysis is a prerequisite (Candès and Donoho, 1999).

The continuous curvelet transform (CCT) can be defined by a pair of windows $W(r)$ (a radial window) and $V(t)$ (an angular window) with variables W as a frequency-domain variable, and r and θ as polar coordinates in the frequency-domain. The admissibility condition as follows should always be obeyed.

$$\sum_{j=-\infty}^{\infty} W^2(2^j r) = 1, \; r \in \left(\frac{3}{4}, \frac{3}{2}\right), \tag{3.1}$$

$$\sum_{j=-\infty}^{\infty} V^2(t-1) = 1, \quad t \in \left(-\frac{1}{2}, \frac{1}{2}\right). \tag{3.2}$$

A polar "wedge" represented by U_j is supported by the radial and angular windows, *W* and *V*. U_j is defined in the Fourier domain by

$$U_j(r,\theta) = 2^{-\frac{3j}{4}} W(2^{-j}r) V\left(\frac{2^{int(\frac{1}{2j})}\theta}{2\pi}\right) \tag{3.3}$$

Where $int(1/2j)$ is the integer part of $(1/2j)$. The polar "wedge", W and V are applied with scale-dependent window widths in each direction.

Define φ_j as a "mother" curvelet and all the curvelets at scale 2^{-j} are derived by rotations and translations of φ_j . Fourier transform $\hat{\varphi}_j(\omega) = U_j(\omega)$ was done in order to define the waveform $\varphi_j(x)$.

The curvelet transform can be defined as a function of $x = (x1, x2)$ at scale 2^{-j}, orientation θ_l, and position $X_k^{(j,l)}$ by

$$\varphi_{j,i,k}(x) = \varphi_j\left(R_{\theta_l}\left(x - x_k^{(j,l)}\right)\right) \qquad \forall\ k = (k_1, k_2) \in Z^2 \tag{3.4}$$

Where k is the sequence of translation parameters.

The rotation angel θ_l is an equi-spaced series defined as $\theta_l = 2\pi \cdot int(-1/2j) \cdot l$, with $l = 0,1,2,3 \ldots$ and $0 \le \theta_l < 2\pi$.

$$x_k^{(j,l)} = R_{\theta_l}^{-1}\left(k_1 \cdot 2^{-j}, k_2 \cdot 2^{-\frac{j}{2}}\right) \tag{3.5}$$

Where R_θ is the rotation matrix in θ radians. R_θ^{-1} is the inverse, and

$R_\theta = \begin{bmatrix} cos\theta & sin\theta \\ -sin\theta & cos\theta \end{bmatrix}$ and $R_\theta^{-1} = R_\theta^{-T} = R_{-\theta} = \begin{bmatrix} cos\theta & -sin\theta \\ sin\theta & cos\theta \end{bmatrix}$

A curvelet coefficient is finally defined as:

$$c(j,l,k) = \langle f, \varphi_{j,l,k} \rangle = \int_{-\infty}^{\infty} f(x)\, \overline{\varphi_{j,l,k}(x)} dx \tag{3.6}$$

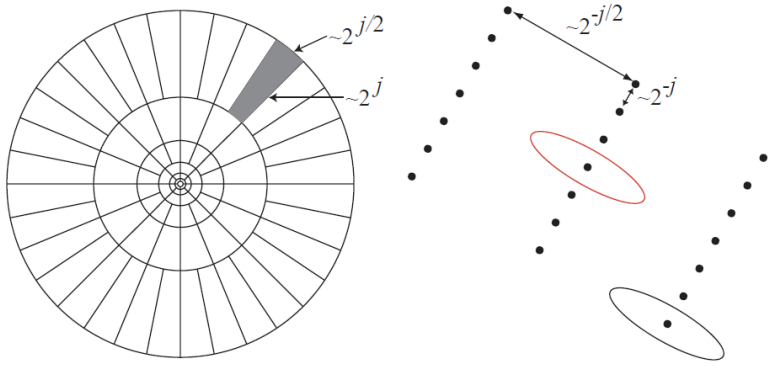

Figure 3.7 Curvelet spatial and angular scale relationship structure (Candès et al., 2006)

Figure 3.7 illustrates the polar "wedges" represented by U_j. The left side of the Figure shows the tilling of the frequency plane. Each ring represents a scale. The amount of directions in each scale which is indicated by the number of "wedges" in each ring depends on the scale. From inside to the outside, the scale is turning from coarser to finer. The Figure on the right side shows grid in a Cartesian reference system. The given orientation and scale is associated with those grids.

❖ Digital curvelet transform

The digital curvelet transform (DCT) in digital coronization, Candès et al. (2006) applied a pseudo-polar grid by revising the window as $\widetilde{W_j}$, which isolates the frequencies near a pseudo-polar wedge (concentric squares, see Figure 3.8). In the Cartesian case, the digital analogue of coefficients can be given by

$$c_\mu = \int \hat{f}(\omega)\, \widetilde{W}_j\left(S_{\theta_l}^{-1}\omega\right) e^{i\langle S_{\theta_l}^{-T} b, w\rangle} d\omega \qquad (3.7)$$

Where , $S_\theta = \begin{pmatrix} 1 & 0 \\ -tan\theta & 1 \end{pmatrix}$ and $b = \left(k_1 \cdot 2^{-j}, k_2 \cdot 2^{-j/2}\right)$.

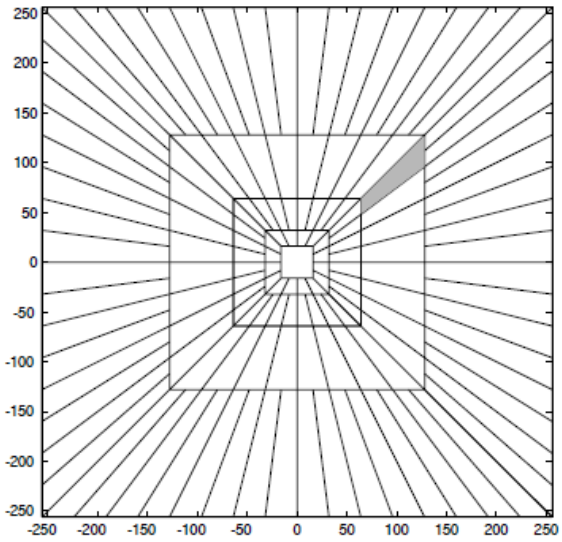

Figure 3.8 The basic tiling of DCT (Candès et al., 2006)

Compared to Figure 3.7, Figure 3.8 is the digital form of the tiling. The windows $\widetilde{W_j}$ smoothly make the Fourier transform localized near the sheared wedges obeying the parabolic scaling. The shaded region represents a typical wedge.

There are two forms of implementing the above mentioned continuous curvelet transform which is defined faithfully by the mathematical transformation (Candès et al., 2006). The first is unequally spaced fast Fourier transformation (USFFT) while the other one is wrapping of the specially selected Fourier samples (wrapping). Since the wrapping version of DCT is faster and has a higher precision in terms of invertible operation (Geback and Koumoutsakos, 2009), only the wrapping version of DCT will be discussed and applied in the following statement.

Since all the applications in this research of DCT are addressed in image processing, instead of considering time domain in signal processing which is originally Candès et al. (2006) consider for, the spatial domain of an image is concerned as the input Cartesian arrays of the form: $f(x_1, x_2)$, $x_1 = 0,1,\ldots,N_1 - 1$, $x_2 = 0,1,\ldots,N_2 - 1$. Where N_1, N_2 represent the width and the height of an image respectively.

The implementation of DCT to a digital image in wrapping version follows the following procedure (Candès et al., 2006):

1. Apply 2D fast Fourier fransformation (FFT) to the image and obtain the samples in the frequency domain.

The discrete transformation form of the image $f(x_1, x_2)$ is:

$$\hat{f}(n_1, n_2) = \sum_{x_1, x_2=0}^{N_1-1, N_2-1} f(x_1, x_2) \cdot e^{-i2\pi\left(\frac{x_1 n_1}{N_1} + \frac{x_2 n_2}{N_2}\right)} \tag{3.8}$$

2. For each scale and angel pair (j, l), calculate the product of $\tilde{\mathrm{U}}_{j,l}(n_1, n_2)\hat{f}(n_1, n_2)$. $\tilde{\mathrm{U}}_{j,l}(n_1, n_2)$ is the localized waveform window.

3. Wrap the product around the origin and get:

$$\tilde{f}_{j,l}[n_1, n_2] = W\left(\tilde{\mathrm{U}}_{j,l}\hat{f}\right)[n_1, n_2] \tag{3.9}$$

4. Get the curvelet coefficient $\mathrm{c}_{jlk} = \langle \hat{f}(n_1, n_2), \hat{\varphi}_{jlk} \rangle$

❖ High-contrast edge detection based on curvelet coefficient

In curvelet domain, the transformed image $f(x, y)$ from the spatial domain is thus represented by curvelet coefficients c_{jlk} in multiple scales and directions. At each space shift k, within one specific scale j, there exist one dominant direction l_m. The dominant direction shows the direction along the main image feature (Geback and Koumoutsakos, 2009). In this research, the dominant direction shows the direction along the curvilinear feature to be extracted.

The fields describing the directions and locations of the curvilinear feature are calculated in the following steps.

1. Select the finest scale which is defined as j_1 and the second finest level defined as j_2 of the transformed curvelet coefficients.

2. Since the curvelet coefficients in scale j_1 and j_2 are not in the same size, it is impossible to overlay them and get the dominant direction unless they are mapped into the same grid size. In addition, the number of angles depends on the scale. Mapping the coefficients in scale j_2 to all the directions in scale j_1 is thus a premise. For mapping the angles from scale j_2 to j_1, the directions in scale j_2 is denoted as l^2 and the mapping function is defined as follows:

$$l^{2'} = floor\left(l^2 \cdot \frac{L_1}{L_2} + 0.5\right) \tag{3.10}$$

Where $l^{2'}$ is the mapped direction in scale j_2. Denote that L_1 and L_2 are the total number of direction in scale j_1 and j_2 respectively.

For each direction l_i^1 $i \in 1,2,3 \dots \mathrm{L}_1$, the size of $c_{j_1 l^1 k}$ is $k_1^{l^1} \times k_2^{l^1}$. For each direction $\mathrm{l}_\mathrm{i}^{2'}$ $\mathrm{i} \in 1,2,3 \dots \mathrm{L}_1$, the size of $\mathrm{c}_{\mathrm{j}_2 \mathrm{l}^{2'} \mathrm{k}}$ is $\mathrm{k}_1^{\mathrm{l}^{2'}} \times \mathrm{k}_2^{\mathrm{l}^{2'}}$.

Similarly, the newly mapped grid $\mathrm{k}_1^{\mathrm{l}^{2'}} \times \mathrm{k}_2^{\mathrm{l}^{2'}}$ is interpolated as:

$$\mathrm{k'}_1^{\mathrm{l}^{2'}} = \mathrm{floor}\left(\mathrm{k}_1^{\mathrm{l}^{2'}} \cdot \frac{\mathrm{K}_1^{\mathrm{l}^1}}{\mathrm{K}_1^{\mathrm{l}^{2'}}} + 0.5\right) \tag{3.11}$$

$$\mathrm{k'}_2^{\mathrm{l}^{2'}} = \mathrm{floor}\left(\mathrm{k}_2^{\mathrm{l}^{2'}} \cdot \frac{\mathrm{K}_2^{\mathrm{l}^1}}{\mathrm{K}_2^{\mathrm{l}^{2'}}} + 0.5\right) \tag{3.12}$$

Denote that $\mathrm{K}_1^{\mathrm{l}^1}$ and $\mathrm{K}_2^{\mathrm{l}^1}$ are the total rows and columns at scale j_1 and in direction l^1 respectively. $\mathrm{K}_1^{\mathrm{l}^{2'}}$ and $\mathrm{K}_2^{\mathrm{l}^{2'}}$ are the total rows and columns at scale j_2 and in direction $\mathrm{l}^{2'}$ respectively.

Since the total number directions, the rows and columns at both scale j_1 and j_2 are the same after mapping, it is possible to overlay them and calculate the dominant direction by adding the coefficients together for each matched direction and grid:

$$\mathrm{M}_{\mathrm{lk}} = \sum_{\mathrm{i}=1,2} \mathrm{c}_{\mathrm{j_i lk}} \tag{3.13}$$

We call M_{lk} the finer scale curvelet magnitude.

For each direction l, we have an unique value of summed curvelet coefficient on each grid k. Find the dominant direction in each grid k by the following equation:

$$l_D(k) = \arg\max M_{lk} \quad , \quad l \in 1,2,3 \dots L_1 \tag{3.14}$$

Thus, the dominant directional field can be defined as

$$\Delta(k) = (M_{l_D k} \cdot cos\theta_{l_D}, M_{l_D k} \cdot sin\,\theta_{l_D}) \tag{3.15}$$

Where θ is defined by the definition of DCT. It is associated with the dominant direction l_D in this case.

Basically, the curvilinear features are represented with the larger coefficients in the high frequency band which is corresponding to the finer scale. We use the non-maximal suppression on finer scale curvelet magnitude along the dominant direction $M_{l_D k}$:

1. Select the curvelet magnitudes $M_{l_D k}$ on grids $(k_1^{l^1}, k_2^{l^1})$ where it has a local maximum across the dominant direction l_D.

2. Use two user defined mark the selected grid k with the curvelet magnitude $M_{l_D k} \geq \mathrm{T}_2$ as "strong" and $\mathrm{T}_1 \leq M_{l_D k} < \mathrm{T}_2$ as "weak". The thresholds are determined by visual interpretation with a trail and error. The extracted curvilinear feature segments shall not be too much so that the noise would be suppressed. It should also not be too little other wise a under estimation will be caused.

3. Select the grids that are marked as "strong" to be considered as the curvilinear feature. For those grids that are marked as "weak", if they are linked with the "strong" grids in any of the 8-neigbour grids, mark it as curvilinear feature as well.

4. The curvilinear feature that detected in by stage 1 to 3 are not always connected. Although the short segments of a complete edge has been handled by the thresholding procedure in stage 3, due to the nearby edges that may influence the local maximum condition of the current edge, it fails to detect the edge completely. By extending the edge along the dominant direction, the gaps between those small segments can thus be bridged. By starting from the end grid of the edge, mark the grids along the dominant directional fields as edge until it reaches to the start grid of another edge segment or the steps set by the user.

5. Since the edge segments that are extracted from the finer scale has the same size as the curvelet coefficients in the finest scale which is $K_1^{l^1} \times K_2^{l^1}$. This is not the size of the original image. The edge map needs to be interpolated in to the original image size. The nearest neighbour method is applied to accomplish the task.

❖ Deleting the small segments

After extracting the preliminary curvilinear feature segments, there are some small segments shown in the circle of Figure 3.9. To delete these small segments, each of the connected components is labelled by a unique ID number. The total amount of pixels that composite each labelled component are calculated. A threshold is then set to delete the components that are consisted by the number of pixels

less than the threshold. Figure 3.10 shows the results of the curvilinear features that are pre-processed and post-processed.

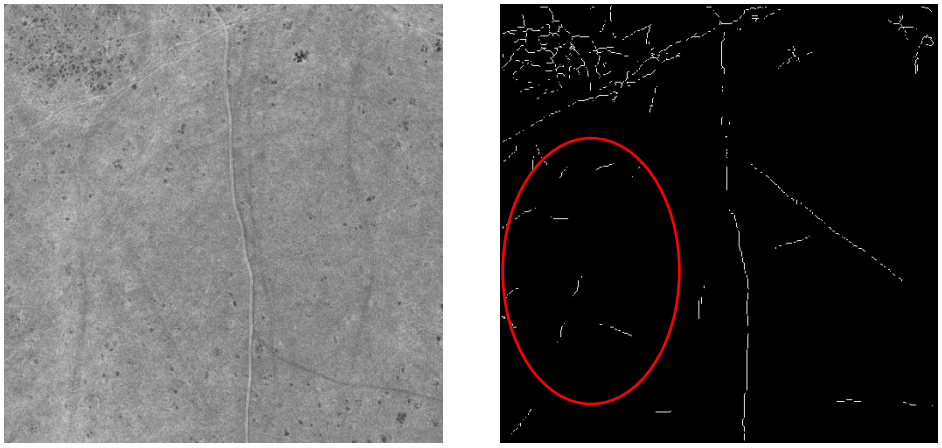

Figure 3.9 The original image comparing with curvilinear feature segments extracted

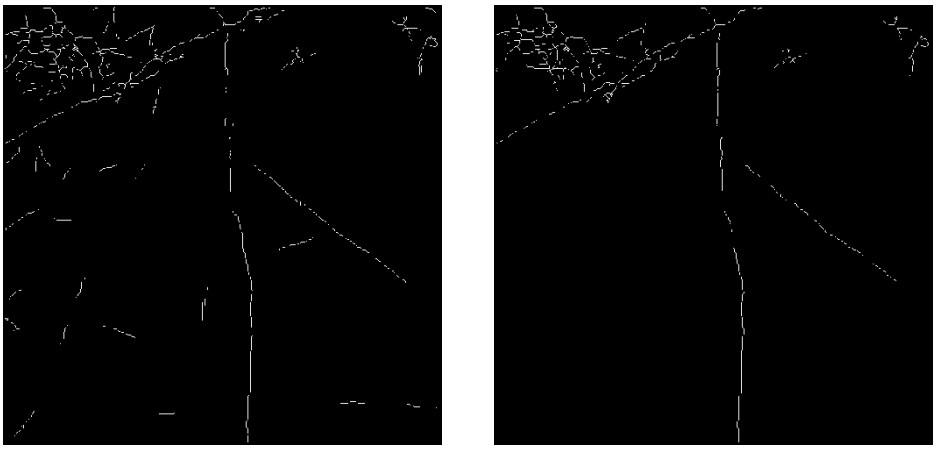

Figure 3.10 The extracted curvilinear feature before and after the small segments filtering

3.3.2 Curvelet-based snake

To find the low-contrast curvilinear features, the enhancement of the low-contrasted curvilinear features should be done in the first place to make it more detectable. Curvelet transform is an edge based multi-scale representation of the image, with the edge information

corresponding to larger curvelet coefficients. Generally, the curvilinear information can be represented with the larger coefficients in the high frequency band. The finer scale, however, usually corresponds to the frequency response of noise and the high-contrast feature; thus the frequency response of the low-contrast edge features should be located at the coarser scale.

After the low-contrast features are enhanced, the non-maximal suppression algorithm is employed again as it is applied for extracting the high-contrast curvilinear feature in section 3.2.

The shape of the low-contrast curvilinear features is rigid due to the scale from where they have been detected. The snake algorithm is further applied to refine the shapes.

❖ Curvelet-based image enhancement

Curvelet coefficients can be modified in order to enhance edges in an image (Starck et al., 2003). For the image in this research a function is defined as follows that is similar to one defined by Starck (2003) with the input curvelet coefficient as x and enhance output of the curvelet coefficient as Y:

$$Y = \begin{cases} 1 & (x < c\sigma) \\ \frac{(x - c\sigma)}{c\sigma} \cdot \left(\frac{m}{c\sigma}\right)^p + \frac{2\sigma - x}{c\sigma} & (x < 2\sigma) \\ \left(\frac{m}{x}\right)^p & (2\sigma < x < m) \\ \left(\frac{m}{x}\right)^s & (x \geq m) \end{cases} \tag{3.16}$$

Where p determines the degree of nonlinearity. s introduces dynamic range compression. A nonzero value of s will enhance the faintest edges and soften the strongest edges at the same time. c is a normalization parameter, and a value larger than 3 guaranties that the noise will not be amplified. The coefficient value that is under m is amplified. This value depends obviously on the pixel values inside the curvelet scale.

In order to not only enhance the curvilinear features of our images but also suppress the background speckle noise, we incorporate hard thresholding into Starck's gain function and obtain the following improved gain function.

$$Y = \begin{cases} 0.01 & (x < c\sigma) \\ 0.005 \times \left[\frac{(x - 0.5\sigma)}{0.5\sigma} \cdot \left(\frac{m}{0.5\sigma}\right)^{p} + \frac{2\sigma - x}{0.5\sigma}\right] & (x < 2\sigma) \\ 0.0001 \times \left(\frac{m}{x}\right)^{0.5} & (2\sigma < x < m) \\ 5 \times \left(\frac{m}{x}\right)^{0.5} & (x \geq m) \end{cases} \quad (3.17)$$

The coefficients are changed from the second coarsest scale to the finest scale. For each scale and within each direction, we calculate the median value of the curvelet coefficients as $\sigma_{jl} = median(c_{jl})$. We also put the max curvelet coefficient in the same scale and same direction as $m_{jl} = max(c_{jl})$ $(\forall\, j = 2,3,4,\ldots, Finest - 1;\ l = 1,2,3,\ldots, L_j)$. L_j is the total number of directions at the scale j.

Since the noise and the background speckle appear in the finest scale, we do not apply the above mentioned Equation (3.17) to change the curvelet coefficient in that scale. Instead, a constant value of 2 has been set to suppress those noises and background speckles. The curvelet coefficients at the coarsest scale $j = 1$ are not transformed but keep them as the original value.

Finally, the image is transformed back into spatial domain by applying the inversed DCT as shown in Figure 3.12. The dark lines are preserved while the background is smoothed and become homogenous. This helps the post stages of processing.

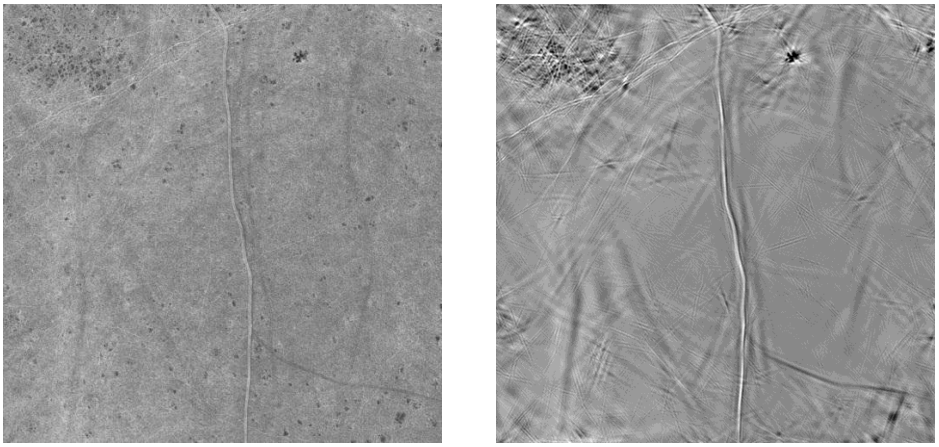

Figure 3.11 Comparison between original image and curvelet-based enhanced image

❖ Finding the low-contrast edge in coarser scale

Although it is a failure to find the significant curvelet coefficient in a finer scale for the low-contrast curvilinear feature, it can be found in a coarser scale as shown in Figure 3.12 below.

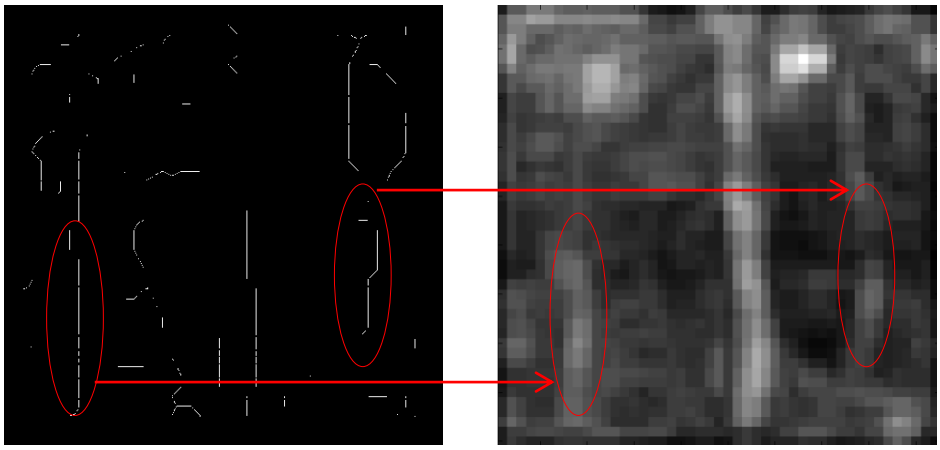

Figure 3.12 Finding edge in coarser scale curvelet magnitude

The similar procedure has been conducted to extract the low-contrast edge as extracting high-contrast curvilinear features in the finer scale described in "High-contrast edge detection based on curvelet coefficient" section.

❖ Refining the shape by Snake

Snake

Snake is a framework that is also called active contour model introduced by Kass et al. (1988). This framework attempts to minimize the energy from the initial contour that is defined by the user while it is evolving itself. The energy of the contour line is a sum of an internal and external energy.

The internal energy relates to the contour geometric property that control the way in which the contour can stretch and curve. Mathematically, it is defined as

$$E_{int} = \alpha \cdot \left|\frac{dv(s)}{ds}\right|^2 + \beta \cdot \left|\frac{d^2v(s)}{ds^2}\right|^2 \tag{3.18}$$

Where $v(s)$ is the set of coordinates of the points that belong to the contour line. The first order derivative: $|dv(s)/ds|$ represents the energy of stretching of the contour line. The higher the value is, the more abrupt the change occurs in the region of the contour spatially. The second order derivative: $|(d^2\, v(s))/(ds^2\,)|$ shows the energy of bending of the contour line. The higher the value is, the greater the curvature of the contour line is. α and β are the weight values of each internal energy partition. Determination of the value of α and β controls the shape of the snake in a way of comprising the stretching and its curvature.

For implementation, the first order derivative can be derived from the following differential equation in the discrete image spatial domain,

$$\left|\frac{dv(s)}{ds}\right| = \sum_{i=1}^{S}\left[\frac{\sqrt{(x_i - x_{i+1})^2 + (y_i - y_{i+1})^2}}{S}\right] - \sqrt{(x_s - x_{s+1})^2 + (y_s - y_{s+1})^2} \quad \forall s \in (1,2,3,\dots,S) \tag{3.19}$$

Where S is the total number of the snake points. The x and y are the pixel coordinates.

The second order derivative can be derived as

$$[d^2\, v(s)/ds^2]^2 = (x_{s+1} - 2x_s + x_{s-1})^2 + (y_{s+1} - 2y_s + y_{s-1})^2 \quad \forall s \in (1,2,3,\dots,S) \tag{3.20}$$

The external energy is also called the image energy. It attracts the contour to low-level features in an image like edges. This energy is supposed to be minimal when the snake is at the object boundary position. Usually, the most common approach is to give low values when the regularized gradient around the contour position reaches its peak value. However, in this research, the aim of using snake is to refine the shape of the low-contrast curvilinear features which are relatively darker than their neighbour background appear in the image. Hence, it is defined as

$$E_{ext} = \gamma \cdot I_{v(s)} \tag{3.21}$$

Where, $I_{v(s)}$ stands for the grey value of the image in pixel whose coordinate is $v(s)$. γ is the weight value for the external energy.

For a set of snake points $v(s)$ the energy function for each single snake point is the summation of the internal energy and external energy:

$$E_{snake}[v(s)] = E_{int}[v(s)] + E_{ext}[v(s)] \quad \forall\, s \in (1,2,3,\dots,S) \tag{3.22}$$

Where S is total number of the snake points.

Define the total energy of the snake which is supposed to be minimized during the self-evolution process as:

$$E_{snake} = \sum_{s=1}^{S}\{E_{int}[v(s)] + E_{ext}[v(s)]\} \quad \forall\, s \in (1,2,3,\dots,S) \tag{3.23}$$

In order to minimize the total snake energy E_{snake}, the set of points on the snake contour need to be evolved by moving to one of its 8-neighbour pixels at each time to recalculate the energy again. This recalculated energy is then compared with the previous one. If the new energy is lower, the evolution will continue to the next step. Otherwise the snake points move to other neighbour pixels and recalculate the energy until the new energy is lower than before. These are done iteratively until the lower energy can not be found or are interrupted by user.

As a short summery of the snake algorithm is shown in Figure 3.13 as a flow chart illustrating the key steps.

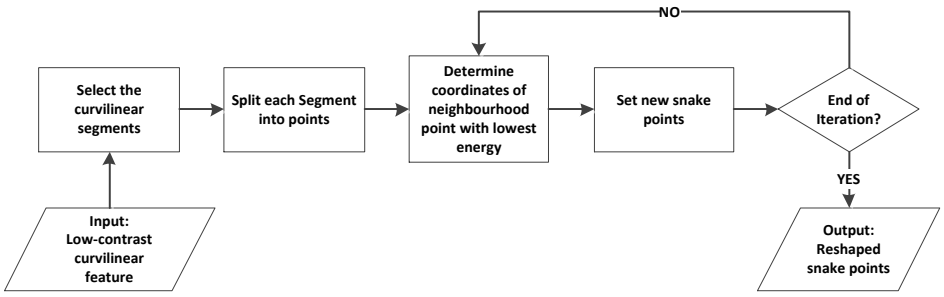

Figure 3.13 A brief flow chart of snake

Snake growing

After the reshaping by snake evolution, the shape of the low-contrast curvilinear feature is no longer rigid. However, there are still some gaps within the curvilinear feature segments as shown in Figure 3.14.

After the ultimate state of snake evolution has been reached and the points on the snake become stable since they have reached to the energy minimum, the growing procedure starts from the end point of each snake line. For each time, there is only one current point created which is several pixels away from the last point. The

determination of each newly glowed point depends on the curvelet-based enhanced image in Figure 3.11. There is a searching window whose size is 11×1 search for the pixel with the lowest grey value

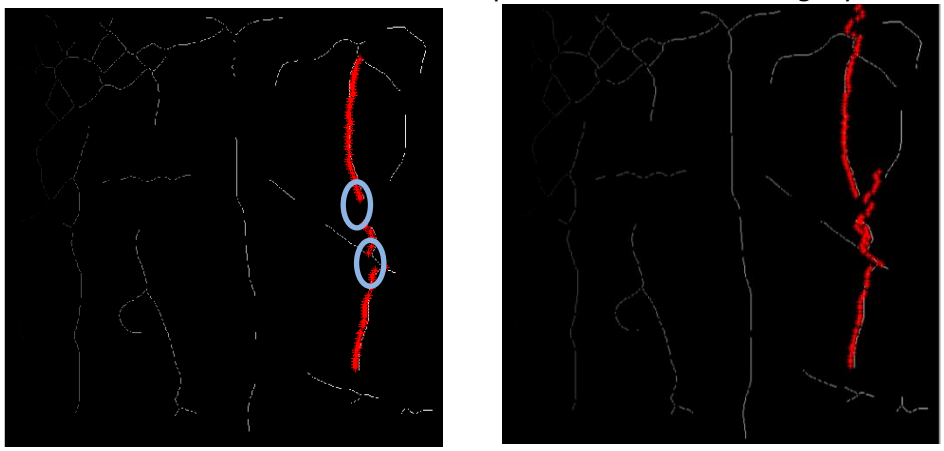

Figure 3.14 Snake points comparison before and after growing

from the curvelet-based enhanced image. This is done iteratively until the stop condition is reached set by the user. Figure 3.14 illustrates how the new snake points look after the growing.

Smoothing with spline fitting

The aim of this procedure is to reconstruct the low-contrast curvilinear feature based on the snake points after growing. The reconstruction mathematical model is a smoothing spline which is a compromise between a linear equation and a third order spline.

$$p\sum_{s}^{S} w_s(a_s - f(s))^2 + (1-p)\int \left(\frac{d^2 f}{ds^2}\right)^2 ds = \text{Min} \qquad (3.24)$$

It is trying to find such a $f(s)$ that minimizes the whole term. $f(s)$ is the mathematics model for the smoothing the snake points. Figure 3.15 shows the smoothed spline fits on the snake points.

❖ Combine the extracted segments from finer and coarser scale

The combination of trails derived from two different procedures is done by overlying the two layers of curvilinear feature segments. Morphological operation "dilate" is used to modify the shape of the segments. Figure 3.16 shows the final results of the extracted trails

from both curvelet coefficient based edge detection approach and curvelet-based snake approach.

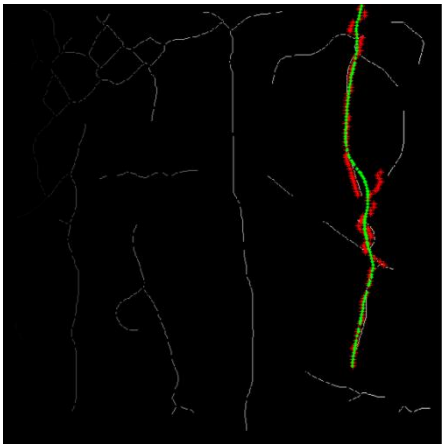

Figure 3.15 Spline fitting for a curvilinear feature segment

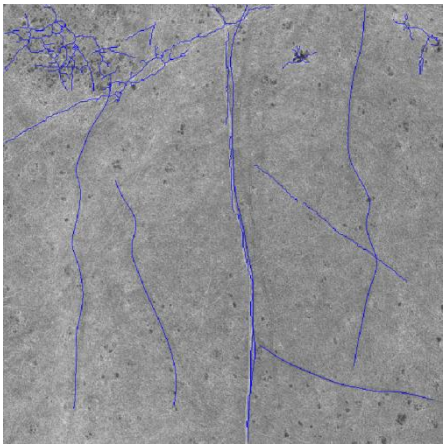

Figure 3.16 Combined trails from both finer and coarser scale

3.3.3 Fuzzy inference-based classification

The trails extracted from the previous steps do not contain any categorical information but just some meaningless curvilinear feature segments. To recognize them needs the computer program simulates human perception of interpreting things. However, in human thinking and language we often use uncertain or vague concepts. Fuzzy inference system is designed for emulating human reasoning when they are classifying things. The following fuzzy logic inference concept

established is based on the text book about GIS applications of fuzzy logic (Kainz, 2002).

❖ Fuzzy set

In general, each extracted but yet to be categorized curvilinear feature segment is an element. And we define two types of trails as two fuzzy sets (vehicle and wildlife trails).

❖ Membership function

It is the membership function that helps each element to decide which fuzzy set it belongs to. It assigns to every element (the curvilinear feature segment) of the universe a degree of membership (or a membership value) to a fuzzy set (a certain type of trail). This membership value must be between zero (no membership) and one (definite membership). All other values between zero and one indicate to which degree an element belongs to the fuzzy set.

❖ Multiple criteria

Criteria can also be considered as indicator for an element to decide itself which fuzzy set it belongs to. However, the indicator can be more than one which make the inference system more robust and act more like an artificial intelligent system. With the multiple indicators, consequently multiple membership functions need to be established. In this research, 3 indicators are considered: cross section profile, length of each curvilinear feature segment and curvelet magnitude.

❖ Fuzzy inference

In this research, the decision is to determine each curvilinear feature segment belongs to either vehicle trail or wildlife trail. The inference system is simply to compare the membership value towards the two fuzzy sets for each segment, the greater the value towards one fuzzy set, the more likely the certain type of trail of that fuzzy set it belongs to. However, since the fuzzy inference system is multiple criteria based different membership values are combined in a convex way which is also known as weighted linear combination (WLC).

❖ Overall procedure of the fuzzy inference system

1. In order to get different indicator value for each segment, for each curvilinear feature segment we sample some of the points on it so that it can keep both efficiency and statistical representative.

2. To get the cross section profile similarity, the idealized profiles designed in section 3.2 are utilized and the actual profile is sampled by taking the cross section pixel values of the sampled points from the original image.

3. The three kinds of indicators are normalized from 0 to 1 so that they are comparable at a same scale.

4. For both types of the trails, build the corresponding membership functions.

5. Make the weighted linear combination for all the membership values and get the ultimate membership value for each of the type of trail.

6. Compare the ultimate fuzzy membership value and make a decision of classification.

❖ The criteria to be considered

✓ Profile matching based criteria

1. Double peak profile

For the typical vehicle trials, they appear double paralleled line in the image whose cross section profiles can be idealized as Figure 3.17 (b). However, their actual cross section profiles look like Figure 3.17 (c).

The similarity between the idealized and the actual is approximate to 1 but can never reach 1.

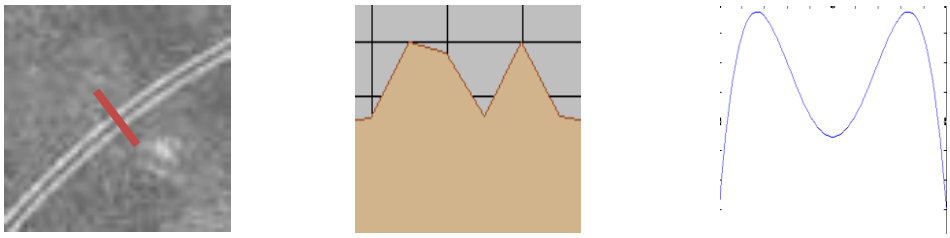

(a) (b) (c)

Figure 3.17 Cross section profile along high-contrast vehicle trail. (a) the original image, (b) actual profile, (c) idealized profile

2. Valley-like profile

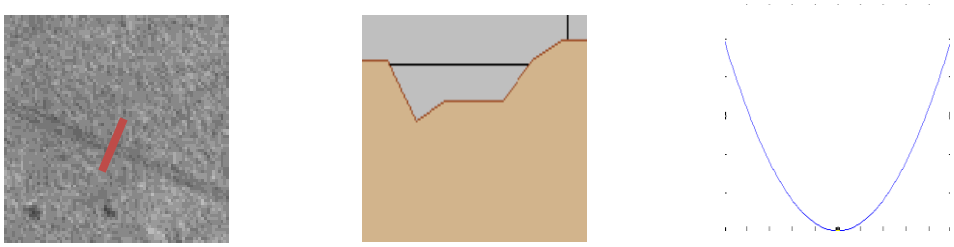

(a) (b) (c)

Figure 3.18 Cross section profile along low-contrast vehicle trail. (a) the original image, (b) actual profile, (c) idealized profile

For the low-contrast vehicle trials, they appear dark line in the image whose cross section profile can be idealized as Figure 3.18 (b). However, their actual cross section profiles look like Figure 3.18 (c).

3. Random profile for wildlife trail

(a) (b)

Figure 3.19 Cross section profile along wildlife trail. (a) the original image, (b) actual profile, (c) idealized profile

For the wildlife trails, they appear as the twisted thread in the image whose cross section profile is random as shown in Figure 3.19 (b).

The similarity measure calculation

The similarity is calculated as the summation of the difference between the grey value of the image in each cross section pixel and the idealized profile value. Here, 11 pixels are considered as a range to establish the profile.

$$S = \sum_{i=1}^{11} |I_i - A_i| \tag{3.25}$$

Where S is the similarity of one curvilinear feature segment to its idealized target cross section profile. I_i and A_i indicate the i^{th} pixel on the cross section profile of the idealized and actual one respectively.

✓ Curvelet magnitude based criteria

The curvelet magnitude derived from section 3.3 is used as another indicator of for each curvilinear feature segment. The motivation behind is the region where the high-contrast vehicle trails occurs is quite brighter than the region where the low-contrast vehicle trails appears in the image. Thus, checking the curvelet magnitude value overlaid with each extracted curvilinear feature segment is an indicator of what kind of trails the segment is. The illustration is shown in Figure 3.20 demonstrating that the difference of curvelet magnitude for different types of trails.

Not all the pixels on the curvilinear feature segment should be considered; otherwise it will affect the efficiency of the whole calculation procedure. Only 5% of the total pixels are considered and the curvelet magnitude values are averaged and normalized to the range of 0-1.

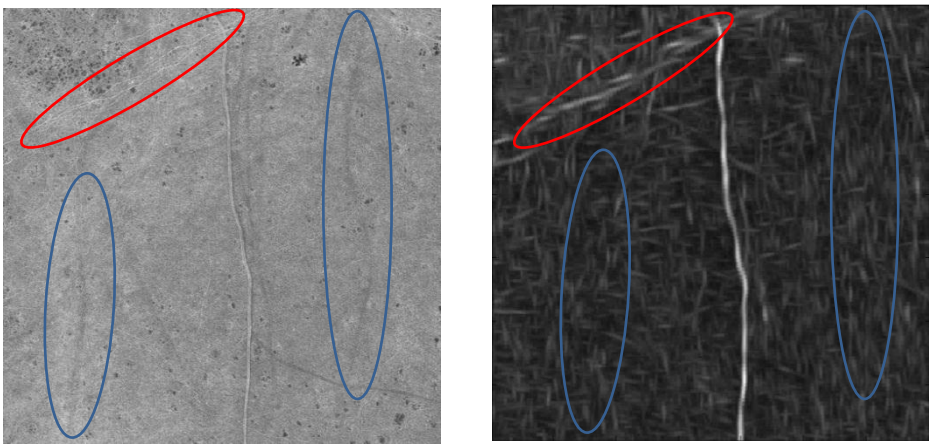

Figure 3.20 Original image and a finer curvelet magnitude image

✓ The segment length criteria

The length of each segment extracted from the previous stages is also considered as the indicator of the types of trails it belongs to. Figure 3.20 shows the types of the trails depends on the length of the curvilinear feature segment. For instance, the wildlife trails appear in the red circle of Figure 3.21 is much shorter than the vehicle trails that beyond the circle.

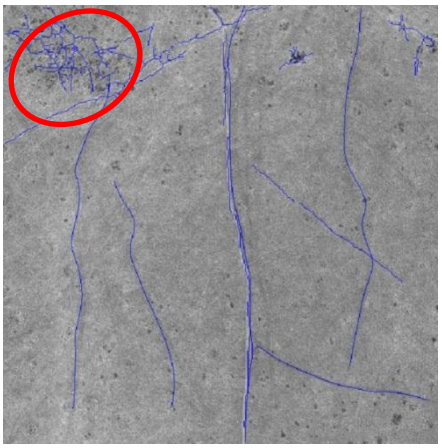

Figure 3.21 All the extracted curvilinear feature segments within the original image

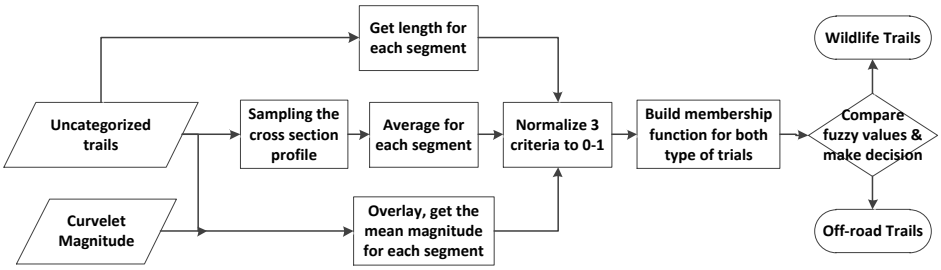

Figure 3.22 The brief flow chart of the fuzzy inference system for this research

❖ Membership function establishment

For different indicators different membership functions are established as follows according to above mentioned justifications:

1. Double peak profile similarity

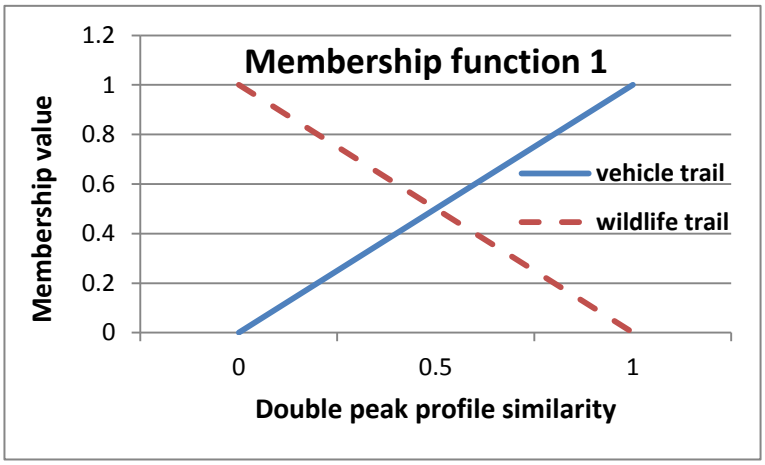

Figure 3.23 Membership function determined by double peak profile similarity

$$\begin{cases} M_{o_1} = Dps & \forall\, Dps \in [\,0,1\,] \\ M_{w_1} = 1 - Dps & \forall\, Dps \in [\,0,1\,] \end{cases} \tag{3.26}$$

Where M_{o_1} is the membership value for vehicle trails and M_{w_1} for wildlife trails. The subscript 1 means the membership value is determined by the first indicator which is the "double peak profile similarity". Dps is the normalized double peak profile similarity value for each curvilinear feature segment.

The more similar the cross section profile of the segment to the double peak shape, the more likely it is the vehicle trail. For wildlife trails whose cross section profile is expected to be random, the higher the similarity value it is, the less chance it is supposed to be vehicle trails. Equation 3.26 are simple linear equations developed based on these facts.

2. Valley-like profile similarity

$$\begin{cases} M_{o_2} = Vps & \forall\, Vps \in [\,0,1\,] \\ M_{w_2} = 1 - Vps & \forall\, Vps \in [\,0,1\,] \end{cases} \tag{3.27}$$

Where M_{o_2} is the membership value for vehicle trails and M_{w_2} for wildlife trails. The subscript 2 stands for the membership value is determined by the second indicator which is the "valley-like profile

similarity". Vps is the normalized valley-like profile similarity value for each curvilinear feature segment.

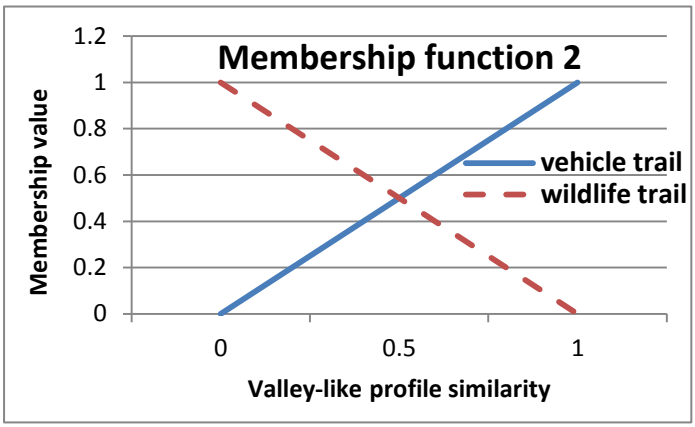

Figure 3.24 Membership function determined by valley-like profile similarity

Since the more similar the cross section profile of the segment to the valley-like shape, the more likely it is the vehicle trail. For wildlife trails whose cross section profile is expected to be random, the higher the similarity value it is, the less chance it is supposed to be vehicle trails. Equation 3.27 are simple linear equations developed based on these facts.

3. Curvelet magnitude

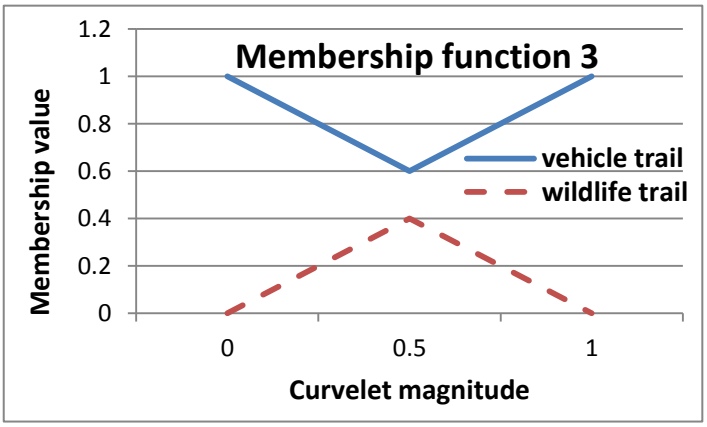

Figure 3.25 Membership function determined by curvelet magnitude

$$\begin{cases} M_{o_3} = -\frac{4}{5}Mag + 1 & \forall\, Mag \in [\,0{,}0.5\,] \\ M_{o_3} = \frac{4}{5}Mag + \frac{1}{5} & \forall\, Mag \in (\,0.5{,}1\,] \\ M_{w_3} = \frac{4}{5}Mag & \forall\, Mag \in [\,0{,}0.5\,] \\ M_{w_3} = -\frac{4}{5}Mag + \frac{4}{5} & \forall\ Mag \in (\,0.5{,}1] \end{cases} \tag{3.28}$$

Where M_{o_3} is the membership value for vehicle trails and M_{w_3} for wildlife trails. The subscript 1 means the membership value is determined by the first indicator which is the "double peak profile similarity". Mag is the normalized curvelet magnitude value for each curvilinear feature segment.

Since there exist two types of vehicle trails (high-contrast and low-contrast) which either has a high curvelet magnitude value or a low curvelet magnitude value, it is effective to use a piecewise function to describe. However, wildlife trails have an intermediate curvelet magnitude. Neither high nor low magnitude value can be regarded as wildlife trails. Equation 3.28 are simple piecewise linear equations developed based on these facts.

4. Segment length

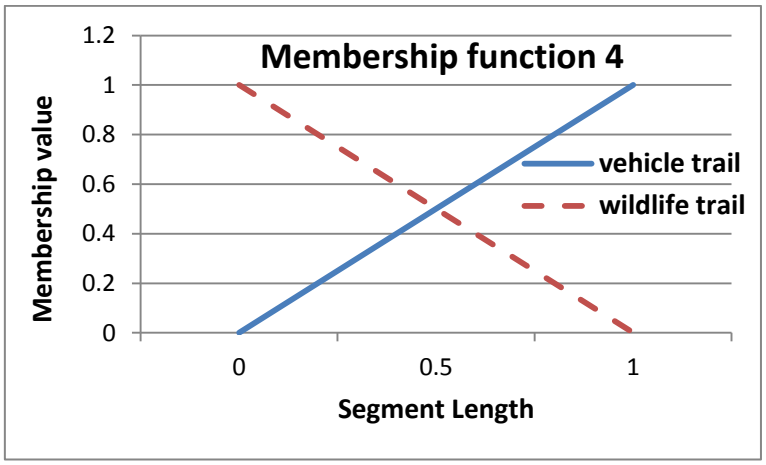

Figure 3.26 Membership function determined by segment length

$$\begin{cases} M_{o_4} = Length & \forall\, Length \in [\,0{,}1\,] \\ M_{w_4} = 1 - Length & \forall\, Length \in [\,0{,}1\,] \end{cases} \tag{3.29}$$

Where M_{o_4} is the membership value for vehicle trails and M_{w_4} for wildlife trails. The subscript 1 means the membership value is determined by the first indicator which is the "double peak profile similarity". $Length$ is the normalized length value for each curvilinear feature segment.

Since the longer the extracted curvilinear feature segment is, the more likely it is the off-road trail. Wildlife trails go to the opposite way. Equation 3.29 are simple linear equations developed based on these facts.

❖ Fuzzy weighted sum combination

Finally, for each curvilinear feature segment the membership values for both wildlife trails and vehicle trails are combined with a corresponding weight.

$$M_o = \frac{\sum_{i=1}^{4}(W_{o_i} \cdot M_{o_i})}{\sum_{i=1}^{4} W_{o_i}} \qquad \forall\, i = 1,2,3,4 \tag{3.30}$$

$$M_w = \frac{\sum_{i=1}^{4}(W_{w_i} \cdot M_{w_i})}{\sum_{i=1}^{4} W_{w_i}} \qquad \forall\, i = 1,2,3,4 \tag{3.31}$$

Where M_o and M_w are the overall membership value for vehicle and wildlife trails respectively. W_{o_i} and W_{w_i} are the weights for the i^{th} indictor of vehicle and wildlife driving trails respectively.

❖ Fuzzy inference decision

After getting the overall membership values for both vehicle and wildlife trails, it is the very final step to make a decision to classify each curvilinear feature segment. By simply comparing the membership values that is belong to each segment, a decision is thus made.

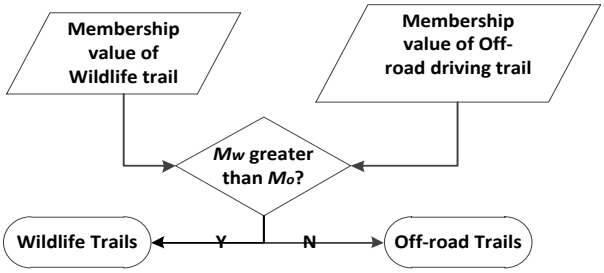

Figure 3.27 The decision procedure of the fuzzy inference system

For each segment, if M_o is greater than M_w, then this segment is categorized as vehicle trail otherwise it should be classified as wildlife trail.

3.4 Validation approach

The validation approach in this research is an adaptation of the methods for evaluation of road extraction proposed by Heipke et al. (1997). Apart from their work, the categorical correctness should also be evaluated which was not an issue for the previous road extraction tasks. Hence, in this research, the categorical error or the categorical quality is added which will be described later. Logically, the validation is separated into two major steps:

1) Matching of the extracted feature with the reference trail network

2) Calculating the quality measures

But firstly the reference data of trails belong to both wildlife and vehicle are digitized manually in ArcGIS based on the GeoEye-1 image panchromatic band.

The extracted and recognized trails are also converted to vector polyline so that they can be overlaid and analysed with the reference data afterwards.

❖ Matching of the extracted feature with the reference data

Matching the extracted data with the reference data is done in a so called "buffer method" (Heipke et al., 1997). Basically, creating a buffer zone with a certain distance which is also called "buffer width" for the reference data is the first stage. Secondly, overlay the extracted data with the buffer. Finally, the segments of the extracted that falls within the buffer are thus considered as "matched extraction" and other segments as "unmatched extraction". Similarly, create the buffer zone for the extracted results and consider the reference segments that fall into the buffer as "matched reference" and other segments as "unmatched reference".

The "matched extraction" is also called "true positive" (TP) which address that the curvilinear feature extraction method has indeed detect the trail in the image.

The "unmatched extraction" is also called "false positive" (FP). It shows the extraction hypothesis is incorrect.

The "unmatched reference" is also called "false negative" (FN).

The illustration of the above mentioned terms is shown by Figure 3.28

❖ Quality measures

In this MSc. research, a number of quality measures (Heipke et al., 1997) are defined as follows:

✓ Geometric quality

1. Completeness

It is the percentage of the reference trails that were able to be explained by the extracted trails.

$$Completeness = \frac{the\ length\ of\ matched\ reference}{total\ length\ of\ reference} = \frac{TP}{TP + FN} \quad (3.32)$$

2. Correctness

It represents the percentage of the reference trails that is explained by the extracted trails. It is also the percentage of the extracted trails that fall into the reference buffer.

$$Correctness = \frac{the\ length\ of\ matched\ extraction}{total\ length\ of\ the\ extraction} = \frac{TP}{TP + FP} \quad (3.33)$$

3. Redundancy

It indicates the percentage where the matched extraction is overlaying with itself.

$$Redundancy = \frac{r}{the\ length\ of\ matched\ extraction} \quad (3.34)$$

Where

$$r = the\ length\ of\ the\ matched\ extraction - the\ length\ of\ matched\ reference$$

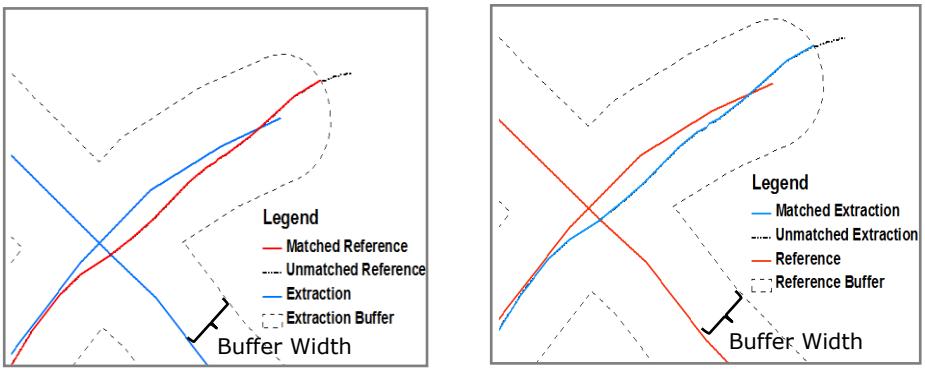

Figure 3.28 Matching principle of validation

✓ Categorical quality

Overlaying the matched extracted trails with the reference buffer does not only provide the information for match length but also the categorical information from their corresponding attribute Table.

An error matrix is a very effective way to evaluate classified map accuracy for land use classification. In this research, this concept is derived for evaluating the categorical extraction quality that is produced by the fuzzy logic inference system developed. The error matrix designed for this research is explained as Table 3.1:

Table 3.1 Error matrix of trails categorization

	Wildlife Trails (m)	**Vehicle Trails (m)**	
Wildlife Trails (m)	$\boldsymbol{n_{11}}$	$\boldsymbol{n_{12}}$	$\boldsymbol{n_{1+}}$
Vehicle Trails (m)	$\boldsymbol{n_{21}}$	$\boldsymbol{n_{22}}$	$\boldsymbol{n_{2+}}$
	$\boldsymbol{n_{+1}}$	$\boldsymbol{n_{+2}}$	**N**

Where n_{ij} denote the number of extracted segments classified into category $i\,(i = 1,2)$ in the extracted trails and category $j\,(j = 1,2)$ in the reference data set. n_{i+} is the number of trail segments classified into category i in the extraction data set. n_{+j} is the number of trail segments that is classified into category j in the reference data set.

The quality measures calculated from the error matrix includes: Overall accuracy and kappa coefficient.

4. Categorical accuracy

This measure is defined as exactly the same as the classification overall accuracy (Congalton, 2009) described in Equation 3.35:

$$Categorical\ accuracy = \frac{(n_{11} + n_{22})}{\sum_{i=1}^{2}\sum_{j=1}^{2} n_{ij}} \tag{3.35}$$

4 Results

In this chapter, three independent test data sets selected in chapter 2 are used to validate the performance of the methods developed in chapter 3. The final extracted results of vehicle and wildlife trails were shown in this chapter both visually and statistically.

After manual digitizing different kinds of trails for each test sets as the reference data, the statistical information is calculated. The overview of length for each trail category is shown in Table 4.1.

Table 4.1 The reference length for each kind of trail in data set 1, 2 and 3

Test Set	Wildlife Trails (m)	Vehicle Trails (m)	Regular Roads (m)	Total Length (m)
1	4520	3882	925	9327
2	1390	5800	1012	8202
3	845	1240	322	2407

Test data set 1 is dominated by wildlife trails while test set 2 and 3 are mainly contain vehicle trails. Due to the image size of the test sets, the third set has the least length in terms of all kinds of trails. The first and second test sets are the same in size with equivalent length of trails.

4.1 Visual results

The following visual results for each test data set composed of both reference data which is digitized manually and the extracted results. Figure 4.1 (a) shows the reference trail map for test data set 1 while Figure 4.1 (b) shows the extraction results. Figure 4.2 (a) and (b) are the trail map for test data set 2 from manual digitizing and extraction algorithms respectively. Reference and extracted trail maps for test data set 3 are shown in Figure 4.3 (a) and (b).

In Figure 4.1 (b), it generally captures the major skeleton of Figure 4.1 (a). However, there are some minor misinterpretations in the lower part of the map which confused the wildlife trail with the vehicle trails. It also misses some vehicle trails. In Figure 4.2 (b), there are more fragmented segments than in the other two data sets. Visually Figure 4.3(b) shows the best matching but some of the vehicle trails are over curved.

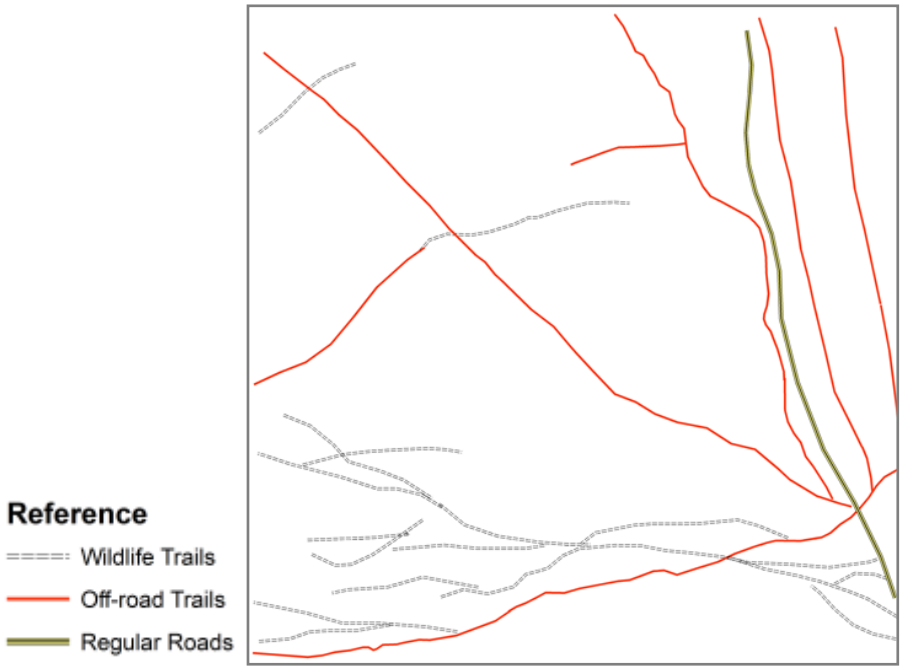

Figure 4.1 (a) Reference trail data for test set 1

Figure 4.1 (b) Extracted trail data for test set 1

Figure 4.2 (a) Reference trail data for test set 2

Figure 4.2 (b) Extracted trail data for test set 2

Figure 4.3 (a) Reference trail data for test set 3

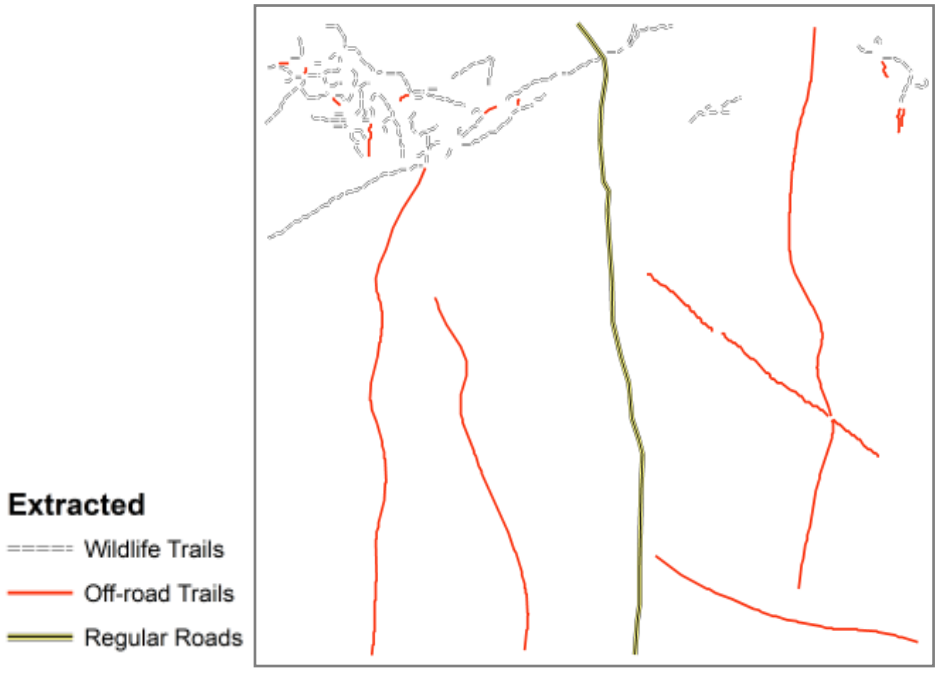

Figure 4.3 (b) Extracted trail data for test set 3

4.2 Statistical results

After the buffer zone overlaying analysis in ArcGIS for both extracted trails and reference trails, the statistical information about the extraction quality and accuracy is shown in the following tables.

Set 1

The matched and unmatched trails statistical information of both extracted and reference data explained in the chapter 3 is shown in Table 4.2.

Table 4.2 Basic statistics for test data set 1

Set 1	Extraction (m)	Matched Extraction (m)	Unmatched Extraction (m)	Matched Reference (m)	Unmatched Reference (m)
Wildlife	3187	3090	97	3340	1180
Vehicle	3874	3425	449	2943	939
Total	7061	6515	547	6283	2119

The error matrix in Table 4.3 shows the performance of the fuzzy inference system for data set 1.

Table 4.3 Categorization error matrix for test data set 1

Extraction/ Reference	Wildlife Trails (m)	Vehicle Trails (m)	Row Total (m)	User
Wildlife Trails (m)	2237	905	3142	71%
Vehicle Trails (m)	853	2520	3373	75%
Column Total (m)	3090	3425	6515	/
Producer	72%	74%	54%	73%

Table 4.4 Quality measure for data set 1

	Correctness	Completeness	Redunancy	Categorical Accuracy
Set 1	**92.3%**	**74.8%**	**3.6%**	**73.0%**

Set 2

The matched and unmatched trails statistical information of both extracted and reference data is shown in Table 4.5.

Table 4.5 Basic statistics for test data set 2

Set 2	Extraction (m)	Matched Extraction (m)	Unmatched Extraction (m)	Matched Reference (m)	Unmatched Reference (m)
Wildlife	**1913**	**1412**	**499**	**642**	**748**
Vehicle	**4409**	**3540**	**869**	**4502**	**1298**
Total	**5585**	**4952**	**633**	**5145**	**2045**

The error matrix in Table 4.6 shows the performance of the fuzzy inference system.

Table 4.6 Categorization error matrix for test data set 2

Extraction/ Reference	Wildlife Trails (m)	Vehicle Trails (m)	Row Total (m)	User
Wildlife Trails (m)	**291**	**468**	**759**	**62%**
Vehicle Trails (m)	**1121**	**3072**	**4193**	**73%**
Column Total (m)	**1412**	**3540**	**7582**	**/**
Producer	**20%**	**87%**	**/**	**68%**

The whole 4 quality measure defined in chapter 3 is shown by Table 4.7.

Table 4.7 Quality measure for data set 2

	Correctness	Completeness	Redunancy	Categorical Accuracy
Set 2	**88.8%**	**71.6%**	**3.9%**	**68.0%**

Set 3

The matched and unmatched trails statistical information of both extracted and reference data is shown in Table 4.8.

Table 4.8 Basic statistics for test data set 3

Set 3	Extraction (m)	Matched Extraction (m)	Unmatched Extraction (m)	Matched Reference (m)	Unmatched Reference (m)
Wildlife	**830**	**612**	**218**	**801**	**44**
Vehicle	**1116**	**1074**	**42**	**986**	**254**
Total	**1946**	**1686**	**260**	**1787**	**298**

The error matrix in Table 4.9 shows the performance of the fuzzy inference system for data set 3.

Table 4.9 Categorization error matrix for data test set 3

Extraction/ Reference	Wildlife Trails (m)	Vehicle Trails (m)	Row Total (m)	User
Wildlife Trails (m)	**612**	**41**	**653**	**94%**
Vehicle Trails (m)	**0**	**1033**	**1033**	**100%**
Column Total (m)	**612**	**1074**	**1686**	**/**
Producer	**100%**	**96%**	**/**	**98%**

The whole 4 quality measure is shown by Table 4.10.

Table 4.10 Quality measure for test data set 3

	Correctness	Completeness	Redunancy	Categorical Accuracy
Set 3	**86.6%**	**85.7%**	**6.0%**	**97.6%**

Overall assessment for 3 data sets

Since we tested 3 different data sets, to make the evaluation more objective, it is necessary to calculate an overall quality measure for assessing the performances of the developed methods. Table 4.11 shows the summary of all the quality measures for each of the test data set as well as the weighted average of them as an overall quality measure. The total length of trails in each test data set is considered as the weight.

Table 4.11 Summary of the quality measures

	Length (m)	Correctness	Completeness	Redunancy	Categorical Accuracy
Set 1	**8402**	**92.3%**	**74.8%**	**3.6%**	**73.0%**
Set 2	**7190**	**88.8%**	**71.6%**	**3.9%**	**68.0%**
Set 3	**2085**	**86.6%**	**85.7%**	**6.0%**	**97.6%**
Overall	**17677**	**90.2%**	**74.8%**	**4.0%**	**73.9%**

5 Discussion

5.1 The strength of this work

To address the strength of the work by comparisons with other's work can difficult be done externally. This is a pity since the similar feature extraction has never been considered in the previous researches or studies. In addition, even though we assume that the wildlife and vehicle trails extraction has been tried before the methods that they might have used must be totally different from this research which made the comparison even challenging.

However, for decades the man-made road extraction has been studied and the accuracy assessment by same quality measures proposed by Heipke et al. (1997) have been reported. Among them, the accuracy assessment results are shown in Table 5.1 (Mayer et al., 2006; Silva et al., 2010; Q. Zhang, 2006). The results shown in the original articles are separated into several groups of different test images and different approaches. To simplified them and make it easily to be compared with the results from this research, all the measures from different sets of imagery and approaches are averaged. The corresponding quality measures for this research are also listed in Table 5.2.

Table 5.1 Comparing average extraction quality from representative road extraction and the trail extraction quality of this research

	Zhang (2006)	Mayer et al. (2006)	Silva et al. (2010)	This research
Completeness	70%	74%	91%	90%
Correctness	56%	72%	78%	74%

In spite of many differences in all kinds of aspects for the traditional man-made road extraction and wildlife or vehicle trails, the results from this research show that it can be an indicator to draw a conclusion that the results and the performance of the developed methods is prospering considering the fact that the complexity and variability of the trails appear in the image. The comparisons still seem insufficient due to the categorical quality. However, the categorical quality is not comparable to any existed research. This is not only because of the uniqueness of objects that have been classified but also the evaluation approach is innovative. Although neither the concepts of fuzzy logic inference system nor error matrix are new, the way this research has used in is total unprecedented.

5.2 The complexity of the study area

Based on the statistical results shown in Table 4.13, it is surprisingly delightful to notice that the test data 3 achieves a very high standard quality in terms of high marks in all aspects of the quality measures. Test data sets 1 and 2 shared same relatively fair quality level with similar quality measure values. This phenomenon can be explained by the complexity of the trails itself as well as their background.

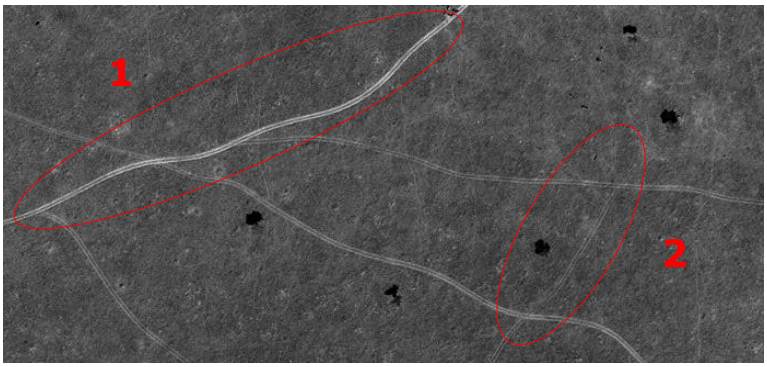

Figure 5.1 The variability of vehicle trails in data set 1

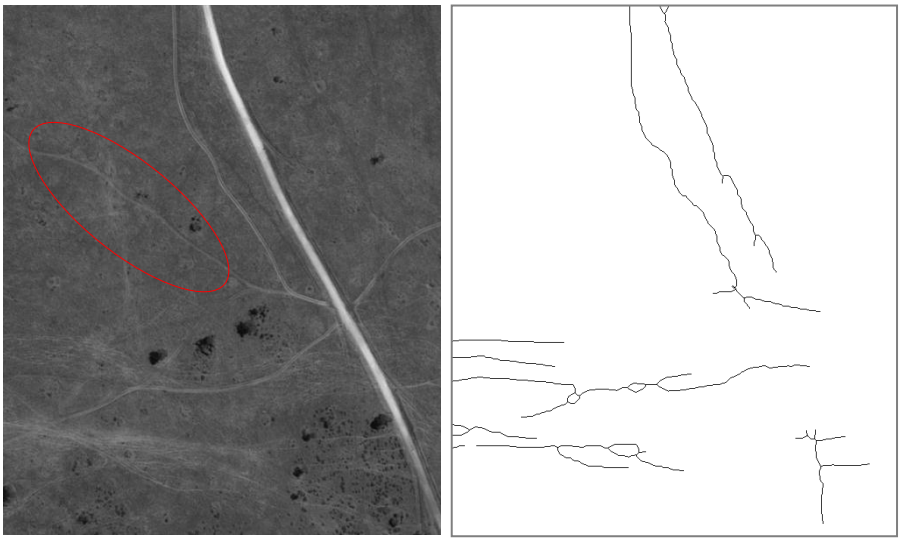

(a) (b)

Figure 5.2 (a) The complexity of different kinds of trails from data set 2, (b) Incomplete extraction of the trails

In Figure 5.1, due to the different frequency of trail usage, the soil condition on the ground or the soil moisture, the brightness of the vehicle trails varies a lot even though they all appear double parallel curvilinear features in the image. Trails in ellipse 1 and 2 are the two cases of the extreme contrast to their background as shown in Figure 5.1. This variability together with the complexity of the trails among different types contributes to the incompleteness of the extraction. To be more specific, the variability and the complexity of the feature in the image lead to the high variability in curvelet domain. This actually makes it difficult to detect all the features completely. Figure 5.3 (b) illustrates the reason that makes the completeness quality measure relatively low for data set 1 and data set 2. Here, the curvelet magnitude inside the ellipse appears much darker as it is supposed to be. Figure 5.3 (a) shows the corresponding original image in an enlarged view showing the difference of the trails to the typical double parallel line vehicle trail.

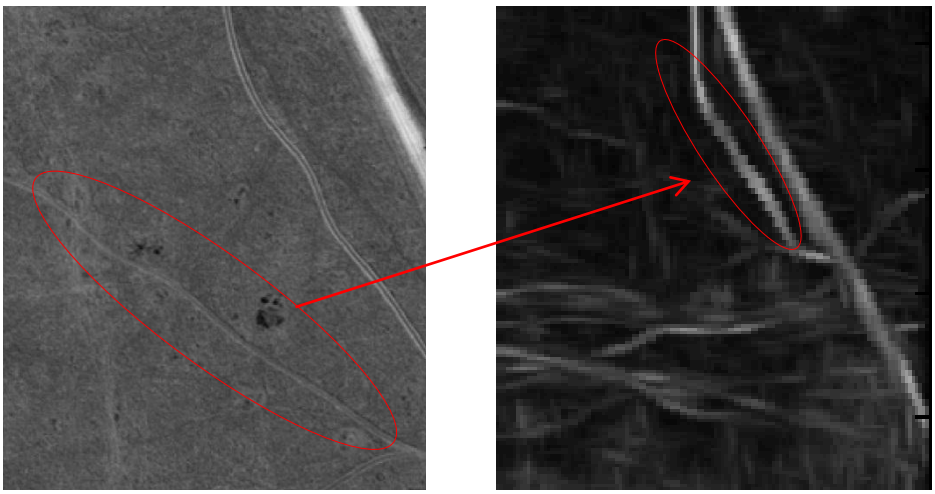

(a) (b)

Figure 5.3 (a) Enlarged original image from data set 2, (b) Curvelet magnitude corresponding to Figure 5.2 from data set 2.

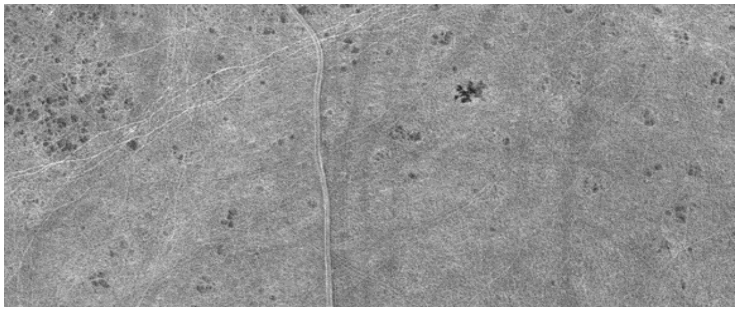

Figure 5.4 Original image from data set 3

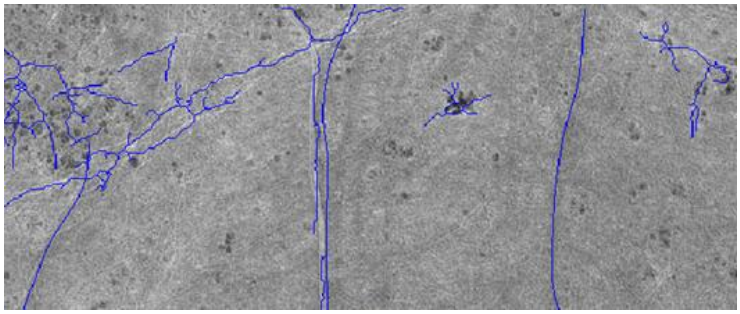

Figure 5.5 Extracted trails overlaid with original image

However, for test data set 3 the trails do not have that much variability and complexity as shown in Figure 5.4. Thus, the extraction is much more complete as shown in Figure 5.5.

5.3 Improvement of the work

Like all the other computer vision and image analysis algorithms, the performance can never be perfect. Since the wildlife and vehicle trails are extracted in such a multiple procedure approach described in chapter 3, the error occurs in each step is propagated in an accumulative manner. To improve the accuracy of the results, the sources of error need to be analysed and the error propagation are broken down as follows. The errors are not simply in both geometric and categorical aspect but also in the evaluation procedure which is easily to be ignored. The evaluation could be improved by line intersect sampling developed by Skidmore and Turner (1992). The following analysis of the sources of improvement is not in a quantitative but in a qualitative manner.

5.3.1 Sources of geometric accuracy error

❖ **Threshold of curvelet-based edge detection**

As described in chapter 3.3.1 the non-maximal suppression of curvelet magnitude for extracting edge in a finer scale depends on the threshold T_1 and T_2 to mark the selected grid k with the curvelet magnitude $M_{l_D k} \geq T_2$ as "strong" and $T_1 \leq M_{l_D k} < T_2$ as "weak". The lower the threshold T_1 and T_2 are set, the more curvilinear feature segments will be extracted. This will cause false positive which will decrease the "correctness" measure. However, if the thresholds are set too high the "completeness" will be decreased. It seems a compromise between the "correctness" and "completeness" by setting different threshold, but considering the potential applications in this research, the "correctness" is more important. It is always acceptable to underestimate some off-road trails which are not so obviously appear in the image. Because those trails are newly created or not often used and this will not have as much impact as the trails that has been frequently used. Underestimating wildlife trails is also not a big issue since the large scale movement of wildlife such as great migration patterns are meaningful to ecologist and animal behaviour researchers.

❖ **Curvelet denoising**

The denoised image as the external energy for the snake points to evolve has a direct impact on the snake shaping. The parameters set for the adapted gain function 3.17 are an outcome after plenty of times of trial and error. Obviously, different people will set different parameters according to their personal preferences. The actually influence of the parameter setting depends on other setting which is discussed in the following section—the snake internal and external energy weight.

❖ **Snake reshaping**

In order to detect the low-contrast curvilinear features in the image snake is introduced in this research. However, there are some parameters need to be set. Amongst the weight for snake internal and external energy is the most important two. The compromise between smoothness of the shape and the proximity of the snake towards the low-contrast curvilinear features is considered being influenced by the application. It is not that important to estimate the shape of the shape very accurately but the location of the low-

contrast curvilinear feature is crucial. Thus the weight of the external energy is put more.

❖ **Snake growing**

Although the snake growing can bridge the gaps of two curvilinear feature segments which considered as the same trail as illustrated in Figure 3.15, it is can also introduce the geometric error especially when the underlying denoised image is not so clear. Figure 5.6 shows the imperfect of the snake points after growing.

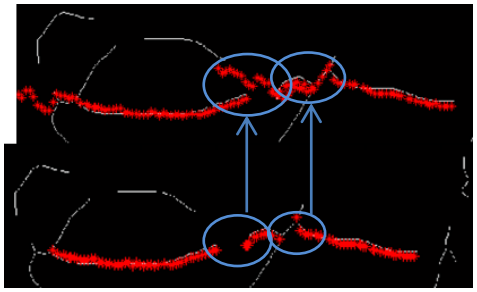

Figure 5.6 Snake points before and after growing

❖ **Spline fitting**

Fitting does not introduce much error as long as the snake points after growing are smooth enough.

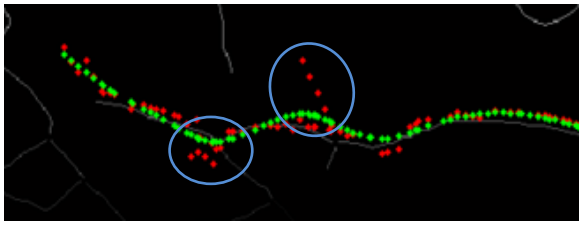

Figure 5.7 Spline fitting of post-growing snake points with outliers

However, there are always some outliers among the snake points. Influenced by those outliers, the fitted shape tries to be attracted to those outliers which degrade the geometric quality as shown in Figure 5.7. Then again, considering the potential application, the error is acceptable since it is not for purpose of the topographic maps.

❖ **The combination of coarse and finer scale**

It is not the combination itself introduces the error but the morphological operator employed.

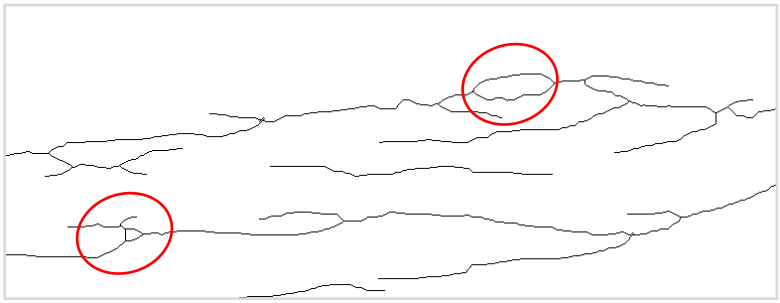

Figure 5.8 The geometric error of extracted wildlife trails caused by morphological operation

As shown in the red circle of Figure 5.8, this kind of error does not have a significant impact on the error evaluation because of they only contribute to the shape imperfection in a very small scale and do not affect the interpretation of wildlife behaviour in a large scale.

5.3.2 Sources of categorical error

❖ **The indicators**

The similarity measures of different cross section profiles are calculated in such a simplified way that only the difference between the template and the actual sample is considered. In some of the cases, the different types of profile may get a high similarity to each other and leads a misclassification in the end.

In general, the vehicle trails are longer than the wildlife trails. However, due to the imperfection of the extraction, there exist some fragments belonging to the vehicle trails. Their length is almost as the as the wildlife trails which confuses the categorization. Figure 5.9 shows the fragmented curvilinear features which are vehicle trails.

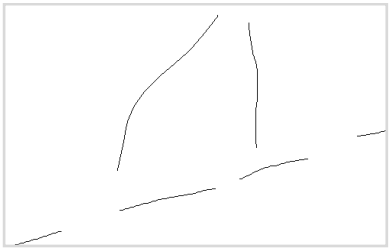

Figure 5.9 Fragmented vehicle trails due to the imperfection of extraction

❖ **Membership functions**

The membership functions for both wildlife and vehicle trails are a series of simplest linear functions. These functions can only represent the fuzziness in a general way. To improve the classification performance, more complicated function should be established which also require plenty of experimental works. Due to the time limitation for this MSc. research, it is not possible to make the function so representative but as a newly established concept to bridge the gap in this research field.

5.3.3 Sources of error from evaluation

❖ **Reference data**

The reference data is the digitized manually. However, digitizing trails in this research is different from digitizing man-made roads in image or linear features from the paper map. Since different people will have different opinions on what to digitize and what not to due to the fact of the variability and complexity of the trails.

As shown in Figure 5.10 (a), according to human perception, there supposed to be junction within the red circle. However, some people might think it is not obviously appeared in the image it should not be digitalized while other people hold the opposite point of view. Digitalizing wildlife trails like Figure 5.10 (b) is another confusing task due to the twist thread trails. Some people might think only the general trend of the trails should be digitalized while other people prefer keeping the details as much as possible. These are just two examples of many of the disagreements that people might have when they are digitizing for creating the reference data. With different reference data, the evaluation results will be different.

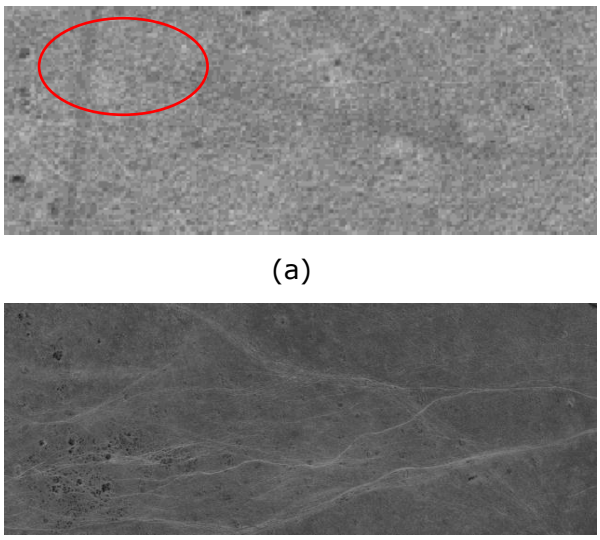

(a)

(b)

Figure 5.10 The variability and complexity of the trails in the image. (a) Low-contrast vehicle trails, (b) Wildlife trails

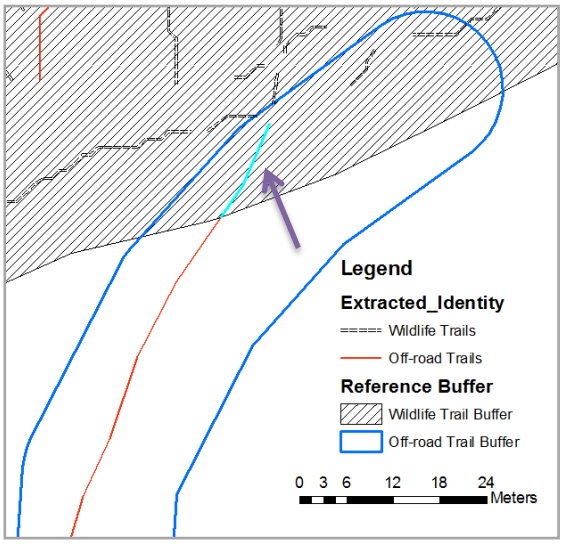

Figure 5.11 Overlapped buffer zone with off-road trail and wildlife trails fall in to them

In addition, in this research, the digitizing work was done by the author who does not have any experience in traveling in Maasai Mara

national reserve. It could be better if we had invited an experienced safari park management expert to do the job, thus the error will be reduced.

❖ **Buffer overlapping**

Since the buffer zones have a certain width, there are some chances for different types of buffer zone to be overlapped with each other as illustrated in Figure 5.11. This may cause error when a certain type of extracted trail falls into the overlapped area like the pointed segment. It is trick to tell whether this segment is categorized correctly or not. Actually, the computer program takes it randomly so the chance is 50%.

❖ **The choice of buffer width**

It is easy to imagine that if the buffer width is too large, false extractions close to the actual trails will be incorrectly considered as the trails. If the width is too small, correct extracted trails with little bit geometric inexact will be rejected which leads a low "completeness" value. Once again, since the ultimate focus on this research is to understand the wildlife migration patterns as well as the current magnitude of vehicle activity, the geometric positional accuracy is not very important.

5.4 Potential ecological applications

For monitoring the off-road driving activities, trail information is very important. As the success of the extraction methods developed in this research, it is very promising to reduce the ecological problems caused by off-road driving activities as raised in chapter one.

Pattern analysis of the trails after being extracted can provide the potential value for ecological applications such as eco-tourism impact studies, for national park management, for the local agencies as well as for researchers who are interested in animal behaviour. However, the kind of pattern should not be only restricted to the density of each kind of trails or the distance between those two kinds. Geometric patterns such as parallel, spark-like, or tree-like can also be analysed. Those patterns may all indicate a certain kind of natural law or reveals a sort of impact that our human beings have caused to nature.

6 Conclusions and recommendations

6.1 Conclusions

Aiming at automatic extraction of never-handled vehicle and wildlife trails with high radiometric variability and a complexity of the back ground from high resolution satellite imagery, an innovative multistage approach has been proposed and implemented by programming. Curvelet transform as the very powerful fundamental tool in the whole research played a key role with its distinct mathematical properties. Dealing with the unprecedented extraction task, new ideas have been incorporated into the existing way of the using curvelet transform in different research fields.

1. Based on Geback and Koumoutsakos's (2009) work on extracting edges in microscopy image for biomedical application purposes, this research extends its core idea and apply it in dealing with both high-contrast and low-contrast curvilinear feature in two different scales in curvelet domain. Thus both types of trails can be extracted effectively.

2. The applications of curvelet transform have been introduced to reduce the speckle noise while enhancing the edge features in SAR (Synthetic Aperture Radar) remote sensing imagery (Ying et al., 2011). Instead of processing directly in the denoised image, the enhanced image is regarded as an external force while applying the snake dealing with low-contrast trails.

3. The fuzzy logic inference concept has been employed by many applications in GIS analysis but has never been used in curvilinear feature categorization. This research filled the blank of curvilinear feature categorization. It also yields the idea of fuzzy logic inference system for trail or more generally, curvilinear feature functionality recognition.

Since the features to be extracted and the methods used in this research are unprecedented, the corresponding evaluation approach is original and based on the approach proposed by Heipke et al. (1997). The categorical quality assessment proposed in this research can be the first of its kind for the evaluation of the similar future research.

The implementation of all the thoughts and ideas in Matlab are successful and the results are satisfactory compared to the other work related to man-made road extractions. However, the three blocks of methods have not been integrated in an organized and systematic way so that it looks like a whole system. For the time being, they are separated as a prototype with no user interface.

6.2 Recommendations

1. Since the curvelet transformation transforms the image into a curvelet domain, the data structure is complicated and the size of the transformed data is a lot of times bigger than the original which require huge amount of time to process. For the time being, with the methods developed in this research it is difficult to handle images larger than 3000*3000 pixels. A more powerful server is needed to handle larger test data set.

2. The whole procedure of the extraction and categorization task can not be fully automated without any human interference. Some parameters need to be set manually based on the results got from the previous stages. Further improvement need to be addressed to make this system more intelligent and fully automated.

3. To improve the impact of the objectivity of validation results, experts from Maasai Mara should be invited to investigate the trails in the image and give advices of digitizing the reference data.

4. To make a better extraction and categorization of the wildlife and vehicle trails, the source of improvement discussed in section 5.3 need to be addressed and provide the corresponding solutions.

5. The different parts of the Matlab code should be integrated with unified input data and output. A user interface should be created and try to code the whole program in C++ language so that it may provide a better performance in terms of computational time and for future commercialization purposes.

References

Bajcsy, R., and Tavakoli, M. (1976). Computer recognition of roads from satellite pictures. *Systems, Man and Cybernetics, IEEE Transactions on, 6*(9), 623-637.

Baltsavias, E. P. (2004). Object extraction and revision by image analysis using existing geodata and knowledge: Current status and steps towards operational systems. *ISPRS Journal of Photogrammetry and Remote Sensing, 58*(3-4), 129-151.

Blaschke, T. (2010). Object based image analysis for remote sensing. *ISPRS Journal of Photogrammetry and Remote Sensing, 65*(1), 2-16.

Bury, R. B. (1980). What we know and don't know about off-road vehicle impacts on wildlife. In P. F. Nowak (Ed.), *Off-road vehicle use: A management challenge* (pp. 110-123): USDA Office of Environmental Quality.

Busack, S. D., and Bury, R. B. (1974). Some effects of off-road vehicles and sheep grazing on lizard populations in the mojave desert. *Biological Conservation, 6*(3), 179-183.

Byoung-Ki, J., Jeong-Hun, J., and Ki-Sang, H. (2002). Road detection in spaceborne sar images using a genetic algorithm. *Geoscience and Remote Sensing, IEEE Transactions on, 40*(1), 22-29.

Candès, E. (1998). *Ridgelets: Theory and applications.* Unpublished Ph.D Thesis, Stanford University, Stanford.

Candès, E., Demanet, L., Donoho, D., and Ying, L. (2006). Fast discrete curvelet transforms. *Multiscale Modeling & Simulation, 5*(3), 861-899.

Candès, E., and Donoho, D. (1999). *Curvelets: A surprisingly effective nonadaptive representation of objects with edges*. Nashville.

Candès, E., and Donoho, D. (2004). New tight frames of curvelets and optimal representations of objects with piecewise c2 singularities. *Communications on Pure and Applied Mathematics, 57*(2), 219-266.

Clement, V., Giraudon, G., Houzelle, S., and Sandakly, F. (1993). Interpretation of remotely sensed images in a context of multisensor fusion using a multispecialist architecture. *Geoscience and Remote Sensing, IEEE Transactions on, 31*(4), 779-791.

Congalton, R. G. (2009). *Assessing the accuracy of remotely sensed data principles and practices*. Boca Raton, FL: CRC/Taylor & Francis.

Couloigner, I., and Ranchin, T. (2000). *Mapping of urban areas : A multiresolution modeling approach for semi-automatic extraction of streets* (Vol. 66). Bethesda, MD, USA: American Society for Photogrammetry and Remote Sensing.

Crist, M. (2006). *Addressing the ecological effects of off-road* The Wildness Society.

Davenport, J., and Switalski, T. A. (2006). Environmental impacts of transport, related to tourism and leisure activities. In J. Davenport & J. L. Davenport (Eds.), *The ecology of transportation: Managing mobility for the environment* (Vol. 10, pp. 333-360): Springer Netherlands.

Dell'Acqua, F., and Gamba, P. (2001). Detection of urban structures in sar images by robust fuzzy clustering algorithms: The example of street tracking. *Geoscience and Remote Sensing, IEEE Transactions on, 39*(10), 2287-2297.

Eckert, R. E., Wood, M. K., Blackburn, W. H., and Peterson, F. F. (1979). Impacts of off-road vehicles on infiltration and sediment production of two desert soils. *Journal of Range Management, 32*(5), 394-397.

Fua, P., and Leclerc, Y. G. (1990). Model driven edge detection. *Machine Vision and Applications, 3*(1), 45-56.

Geback, T., and Koumoutsakos, P. (2009). Edge detection in microscopy images using curvelets. *BMC Bioinformatics, 10*(1), 75.

Goudie, A. (2006). *The human impact on the natural environment: Past, present, and future*: Blackwell Pub.

Griggs, G., and Walsh, B. (1981). The impact, control, and mitigation of off-road vehicle activity in hungry valley, california. *Environmental Geology, 3*(4), 229-243.

Gruen, A., and Li, H. (1997). Semi-automatic linear feature extraction by dynamic programming and lsb-snakes. *PE&RS*(8), 67.

Heipke, C., Mayer, H., Wiedemann, C., and Jamet, O. (1997). *Evaluation of automatic road extraction.* Paper presented at the IAPRS XXXII.

Heipke, C., Steger, C., and Multhammer, R. (1995). *Hierarchical approach to automatic road extraction from aerial imagery.* Paper presented at the Proc. SPIE.

Hinz, S., Baumgartner, A., Steger, C., Mayer, H., Eckstein, W., Ebner, H., Radig, B., and Semantische, S. (1999). *Road extraction in rural and urban areas.* Paper presented at the SMATI'99, Munich.

Ikiara, M., and Okech, C. (2002). *Impact of tourism on environment in kenya : Status and policy* (No. 9966949372 9789966949370). Nairobi, Kenya: Kenya Institute for Public Policy Research and Analysis.

Kainz, W. (2002). Fuzzy logic and gis. 2012, from http://homepage.univie.ac.at/wolfgang.kainz/Lehrveranstaltungen/ESRI_Fuzzy_Logic/File_2_Kainz_Text.pdf

Kass, M., Witkin, A., and Terzopoulos, D. (1988). Snakes: Active contour models. *International Journal of Computer Vision, 1*(4), 321-331.

Kassar, C. (2005). *Motorized recreation at a crossroads: Lessons from the past converge with management practices of the future – off road vehicle use on public lands*. Bishop: Friends of the Inyo.

Knight, R. L., and Gutzwiller, K. J. (1995). *Wildlife and recreationists: Coexistence through management and research*: Island Press.

Koutaki, G., and Uchimura, K. (2004). *Automatic road extraction based on cross detection in suburb.* Paper presented at the Image Processing: Algorithms and Systems III. Edited by Dougherty, Edward R.; Astola, Jaakko T.; Egiazarian, Karen O. Proceedings of the SPIE, Volume 5299, pp. 337-344 (2004).

Lee, T. H., and Moon, W. M. (2002). *Lineament extraction from landsat tm, jers-1 sar, and dem for geological applications.* Paper presented at the Geoscience and Remote Sensing Symposium, 2002. IGARSS '02. 2002 IEEE International.

Marikhu, R., Dailey, M. N., Makhanov, S., and Honda, K. (2007). *A family of quadratic snakes for road extraction*. Paper presented at the Proceedings of the 8th Asian conference on Computer vision - Volume Part I.

Mayer, H., Hinz, S., Bacher, U., and Baltsavias, E. (2006). A test of automatic road extraction approaches. [On CD-ROM]. *International Archives of Photogrammetry, Remote Sensing and Spatial Information Sciences, 36*(3).

Mena, J. B. (2003). State of the art on automatic road extraction for gis update: A novel classification. *Pattern Recognition Letters, 24*(16), 3037-3058.

Mirnalinee, T., Das, S., and Varghese, K. (2011). An integrated multistage framework for automatic road extraction from high resolution satellite imagery. *Journal of the Indian Society of Remote Sensing*, 1-25.

Mnih, V., and Hinton, G. (2010). Learning to detect roads in high-resolution aerial images. In K. Daniilidis, P. Maragos & N. Paragios (Eds.), computer vision – eccv 2010 (Vol. 6316, pp. 210-223): Springer Berlin / Heidelberg.

Mohammadzadeh, A., Valadan Zoej, M., and Tavakoli, A. (2009). Automatic main road extraction from high resolution satellite imageries by means of particle swarm optimization applied to a fuzzy-based mean calculation approach. *Journal of the Indian Society of Remote Sensing, 37*(2), 173-184.

Neuenschwander, W. M., Fua, P., Iverson, L., Székely, G., and Kübler, O. (1997). Ziplock snakes. *International Journal of Computer Vision, 25*(3), 191-201.

Priskin, J. (2003). Physical impacts of four-wheel drive related tourism and recreation in a semi-arid, natural coastal environment. *Ocean & Coastal Management, 46*(1-2), 127-155.

Reigber, A., Jager, M., He, W., Ferro-Famil, L., and Hellwich, O. (2007). *Detection and classification of urban structures based on high-resolution sar imagery.* Paper presented at the Urban Remote Sensing Joint Event, 2007.

Silva, C. R. d., Silva Centeno, J. A., and Henriques, M. J. (2010). Automatic road extraction in rural areas, based on the radon transform using digital images. *Canadian Journal of Remote Sensing, 36*(6), 737-749.

Sindiga, I. (1999). Tourism and african development : Change and challenge of tourism in kenya. African Studies Centre.

Skidmore, A. K., and Turner, B. J. (1992). Map accuracy assessment using line intersect sampling. *PE&RS, 58*(10).

Starck, J. L., Murtagh, F., Candes, E. J., and Donoho, D. L. (2003). Gray and color image contrast enhancement by the curvelet transform. *Image Processing, IEEE Transactions on, 12*(6), 706-717.

Suetens, P., Fua, P., and Hanson, A. J. (1992). Computational strategies for object recognition. *ACM Comput. Surv., 24*(1), 5-62.

Taylor, R. B. (2002). The effects of off-road vehicles on ecosystems. *Texas Parks and Wildlife*.

Tieling, C., Jinfei, W., and Kaizhong, Z. (2002). *A wavelet transform based method for road extraction from high-resolution remotely sensed data.* Paper presented at the Geoscience and Remote Sensing Symposium, 2002. IGARSS '02. 2002 IEEE International.

Walpole, M. J. (2003). *Wildlife and people: Conflict and conversation in masai mara, kenya*: International Institute for Environment and Development.

Webb, R. H., Ragland, H. C., Godwin, W. H., and Jenkins, O. (1978). Environmental effects of soil property changes with off-road vehicle use. *Environmental Management, 2*(3), 219-233.

Wildlands, C. (2011). Recent off-road vehicle scientific research reviews.

Wilson, J. P., and Seney, J. P. (1994). Erosional impact of hikers, horses, motorcycles, and off-road bicycles on mountain trails in montana. *Mountain Research and Development, 14*(1), 77-88.

Vollmer, A. T., Maza, B. G., Medica, P. A., Turner, F. B., and Bamberg, S. A. (1977). The impact of off-road vehicles on a desert ecosystem. *Environmental Management, 1*(2), 115-129.

Vosselman, G., and Knecht, J. (1995). *Road tracing by profile matching and kalman filtering.* Paper presented at the Workshop on Automatic Extraction of Man-made Objects from Aerial and Space Images, Berlin, Germany.

Ying, L., Hongli, G., Dagan, F., and Yanning, Z. (2011). An adaptive method of speckle reduction and feature enhancement for sar images based on curvelet transform and particle swarm optimization. *Geoscience and Remote Sensing, IEEE Transactions on, 49*(8), 3105-3116.

Yuan, G., Zhengyao, B., Yue, L., and Yang, L. (2007, 24-27 Aug. 2007). *Genetic algorithm and region growing based road detection in sar images.* Paper presented at the Natural Computation, 2007. ICNC 2007. Third International Conference on.

Zhang, C., and Baltsavias, E. P. (1999). *Road network detection by mathematical morphology.* Paper presented at the Proc. of International Workshop on 3D Geospatial Data Production, Paris.

Zhang, C., Baltsavias, E. P., and Gruen, A. (2000). Knowledge based image analysis for 3d road reconstruction, *Asian Journal of Geoinformatics* (pp. 3-8).

Zhang, Q. (2006). *Automated road network extraction from high spatial resolution multi-spectral imagery.* Unpublished Phd. thesis, University of Calgary, Calgary, Canada.

Zhang, Q., and Couloigne, I. (2004). *A wavelet approach to road extraction from high spatial resolution remotely-sensed imagery* (Vol. 58). Nepean, ON, CANADA: Canadian Institute of Geomatics.

Zhu, C., Shi, W., Pesaresi, M., Liu, L., Chen, X., and King, B. (2005). The recognition of road network from high-resolution satellite remotely sensed data using image morphological characteristics. *International Journal of Remote Sensing, 26*(24), 5493-5508.

Zlotnick, A., and Carnine, P. D. (1993). Finding road seeds in aerial images. *CVGIP: Image Understanding, 57*(2), 243-260.